WIND-DRIVEN CIRCULATION IN PRINCESS ROYAL HARBOUR:

RESULTS FROM A NUMERICAL MODEL

THE LIBRARY
DEPT. OF CONSERVATION
& LAND MANAGEMENT
- 9 JUN 1993
WESTERN AUSTRALIA

DEPARTMENT OF CONSERVATION AND ENVIRONMENT
PERTH WESTERN AUSTRALIA
Bulletin 229 November 1985

WIND-DRIVEN CIRCULATION IN PRINCESS ROYAL HARBOUR

RESULTS FROM A NUMERICAL MODEL

D.A. Mills and K.M. Brady

DEPARTMENT OF CONSERVATION AND ENVIRONMENT
1 MOUNT STREET
PERTH WESTERN AUSTRALIA

ABSTRACT

The combined influence of bathymetry, wind speed and wind direction on the local wind-induced water circulation of Princess Royal Harbour was examined using a numerical hydrodynamic model. Initially, flows through the harbour entrance were neglected, i.e. the harbour was treated as a closed water body. The results of this investigation showed that north to west winds promote large scale anti-clockwise circulation, and east to south winds favour large scale clockwise circulation. South-west winds generate two counter-rotating gyres. The results also suggest that the rate of flushing of waters on the shallow western margin of the harbour is strongly dependent on wind direction as well as on wind speed. Winds blowing along the length of the harbour and the shallows are much more efficient agents of water replacement than are winds blowing across the shallows, from the south-west.

ISBN 0 7309 0690 6

CONTENTS

FIGURES

TABLES

1. INTRODUCTION

The first permanent European settlement in the south-west of Australia was established in 1826, on the northern shore of Princess Royal Harbour (Figure 1). This settlement formed the early history of Albany, the town which has since grown and spread around the northern and western shores of the harbour.

Princess Royal Harbour (PRH) is an almost land-locked bay situated on the south coast of Western Australia (Figure 1). It is approximately elliptical in shape, being eight kilometres long in a north-west to south-east direction, and four kilometres wide. PRH comprises a deep basin, bordered by a sandy intertidal to subtidal shelf which is most extensive (about 1.5 km wide) off the western and southern shores. The harbour has a narrow opening into King George Sound. Adjacent to this entrance, and to port facilities on the north-east shore, an area has been dredged to twelve metres. No major rivers discharge into PRH; the only sources of fresh water are drainage channels, local runoff and direct precipitation.

Albany supports industries including a superphosphate plant, woollen mills, abattoirs and food processing works. Some of these industries discharge effluents directly into PRH. The harbour acts as a major port and as a base for professional fishing operations. Aside from these uses, the harbour provides recreational opportunities for the residents of Albany, and attracts tourists to the region.

For some years there has been concern over the effects of effluent discharge on the water quality in PRH. In 1978, the Albany Waterways Management Advisory Committee requested that a study of the harbour be carried out to examine the main problem areas and to recommend action. This work was undertaken by the Department of Conservation and Environment in co-operation with the Botany Department of the University of Western Australia, the Public Health Department, and the then Department of Fisheries and Wildlife. The investigation dealt mainly with nutrient and phytoplankton levels, and the bacteriological status of PRH and surrounding waters. It identified the port and the western shallow margin as problem areas for accumulations of bacteria and nutrients, respectively (Atkins, Iveson, Field and Parker, 1980).

More recently it has been found that molluscs, fish and sediments in parts of the western shallow margin of PRH contain high concentrations of heavy metals (Talbot, 1983; Jackson, Gorman, Hancock, Chittleborough and Talbot, 1984). This is the result of discharges over a number of years from a rock phosphate processing plant. The degree of resuspension of the contaminated sediments, and the actual concentrations of heavy metals in the water have yet to be investigated in detail.

One of the major recommendations from the report of Atkins et al (1980) was that "a detailed study of water movement in the harbour and in King George Sound should be made so that nutrient dispersal and accumulation may be fully understood and appropriate management assured." In keeping with this recommendation, and in view of the general lack of oceanographic knowledge for this area, a study has commenced, with the objectives:

- to determine the major characteristics of water circulation and exchange,

- to understand the dispersion and flushing of materials released to these waters, and

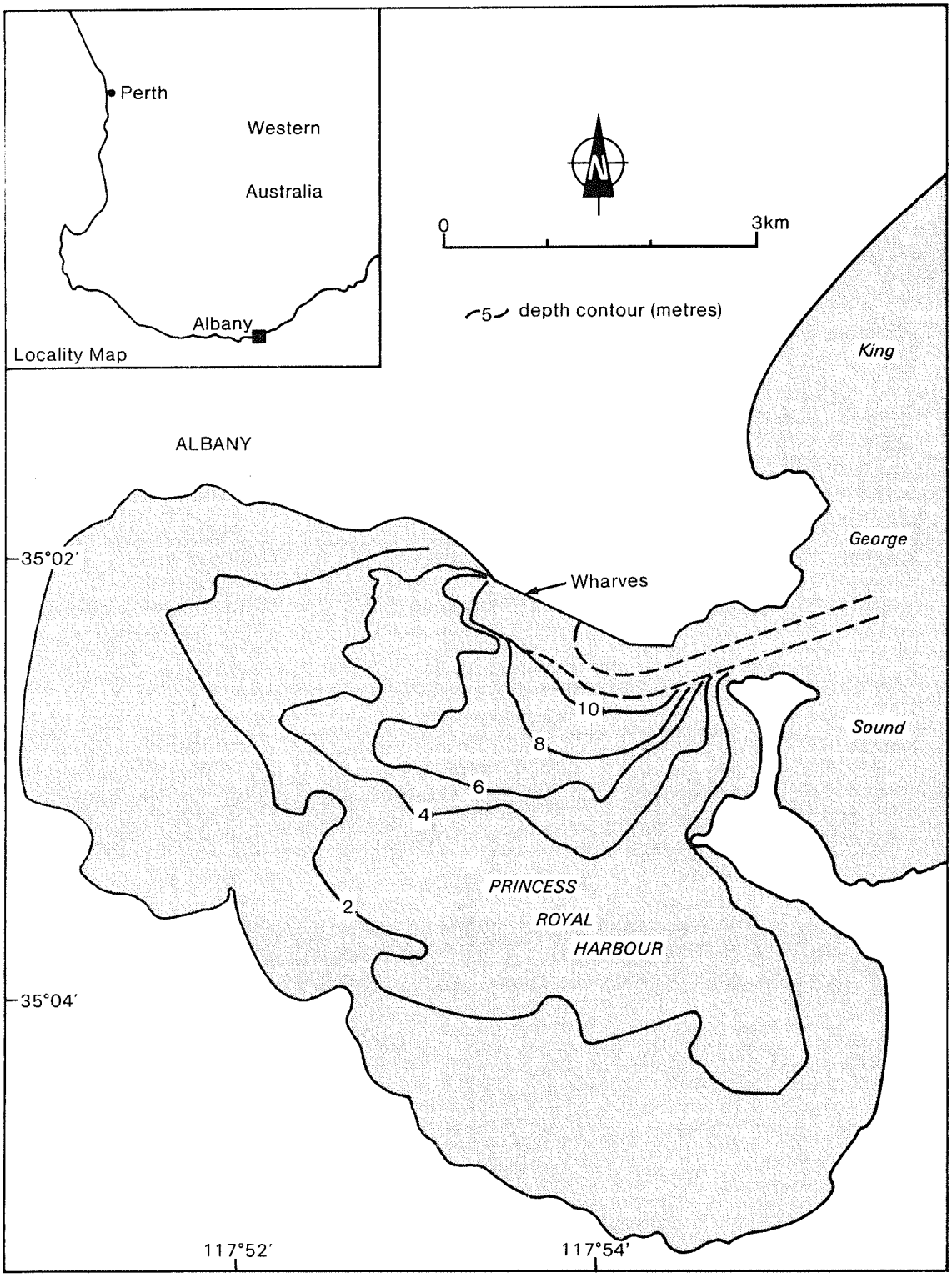

Figure 1 : Princess Royal Harbour, Albany. Location and bathymetry.

- to form a basis for the management of the water quality in this area.

The first phase of the study was focussed on the local wind-induced circulation of PRH waters. A numerical hydrodynamic model was used to calculate depth-averaged currents and surface elevations induced by applied wind stress. Initially the effects of flows through the harbour entrance were neglected. Simple forms of the wind stress were prescribed in order to facilitate examination of:

- the response times of PRH water following the onset of a wind,
- the steady-state current speeds attainable for a given wind stress at any point in the harbour, and
- the nature of the water circulation patterns for winds of different directions.

Knowledge of these basic characteristics aids interpretation of the harbour's response to more complex wind events.

It is recognised that other factors contribute to water circulation in PRH, such as the tides, and local or regional meteorological effects which influence water level and flow through the harbour entrance. These are not addressed in this paper, however they will be considered as the investigation of this region proceeds.

2. METHODS

2.1 The Model

The study made use of a two-dimensional, vertically-averaged, numerical hydrodynamic model, described in Mills (1985). This model employs an explicit, finite-difference numerical scheme to solve the non-linear equations of motion for a water body of known bathymetry. It is assumed that bottom shear stress and depth-averaged velocity may be related. The results presented in this paper were derived with a purely quadratic bottom stress relationship, however an optional linear/quadratic form (e.g. Hunter, 1983) has also been included in the model. Flooding and drying of shallow banks can now be represented by moveable model boundaries, using the method of Flather and Heaps (1975). This feature was required here to simulate the partial exposure of the shallow margins of PRH by strong wind events.

Such models are applicable to well-mixed water bodies where flow variations in the vertical are unimportant. Temperature and salinity data from PRH (Atkins et al, 1980) showed that the harbour is generally well-mixed, particularly in summer. Thus the model should be able to represent the major depth-averaged circulation features of the harbour, especially under conditions of sustained, moderate to strong winds.

2.2 Modelling Procedure

A 300 m grid system was chosen to cover PRH, with one of its axes aligned parallel to the Albany Port Authority shipping wharves (297° N). Data input matrices (dimensions 28 x 17) describing coastal form and water depths were prepared from a 1:15 000 scale chart (Public Works Department, WA OM52923, 1981). Prominent coastline and bathymetric features were well resolved, as shown on Figure 2, which is derived from the input data.

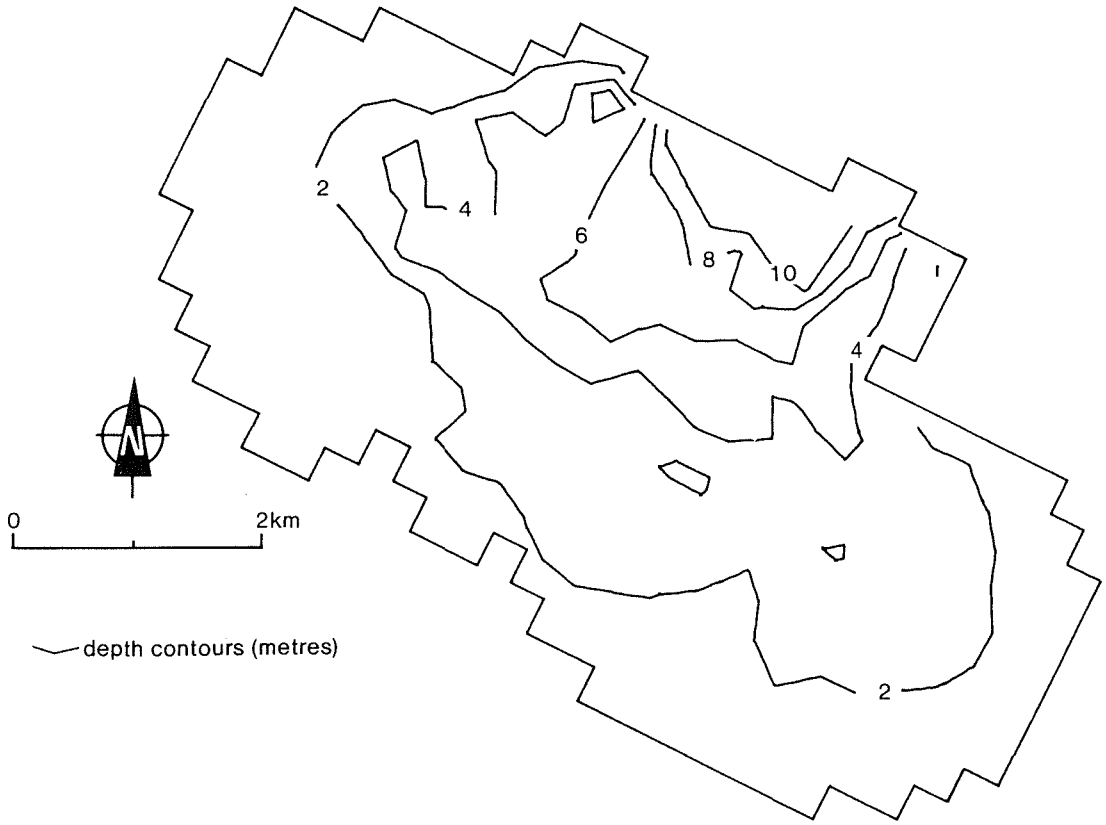

Figure 2 : Model representation of Princess Royal Harbour bathymetry

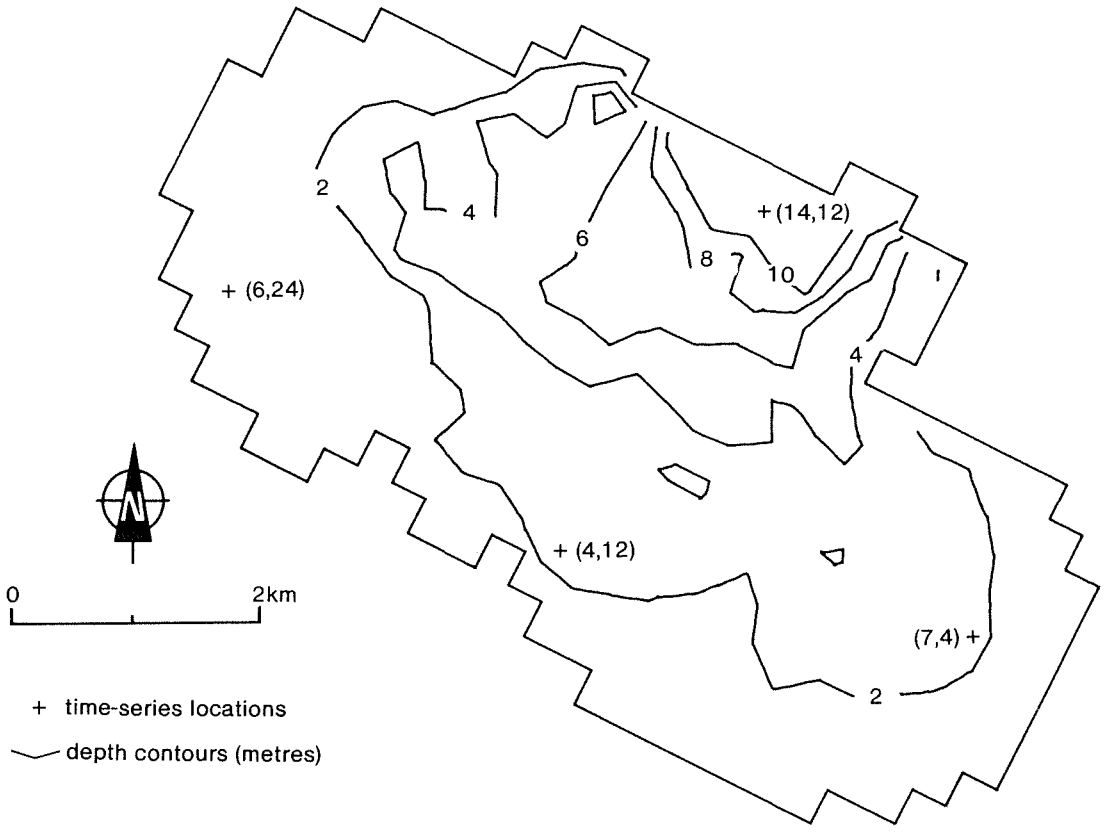

Figure 3 : Model representation of Princess Royal Harbour, showing locations of intensive time-series model results.

At the commencement of each model run the values of elevation and current speed were set to describe an undisturbed water body with horizontal surface level at 0.76 m above chart datum (approximately Australian Height Datum).

PRH was assumed completely closed, and therefore free of dynamic influences related to water levels outside of the harbour, e.g. tidal variations. Thus, at each point around the model boundary, a condition of zero normal flow was specified.

A numerical stability criterion (Courant et al, 1928) imposed an upper limiting value for the computational time step of 18.3s, corresponding to a maximum water depth in the model of 13.6m. The value actually used was 12s, so that 7 200 model time steps represents one day.

The model of PRH was forced by uniform, constant wind stress vector fields, switched on at time t=0. No special measures were required to reduce the size of initial high frequency disturbances arising from the sudden onset of the wind, as these were rapidly damped by bottom friction. All trials included the effects of momentum advection.

A summary of model parameter values used is given:

Grid length	300 m
Time step	12 s
Coriolis parameter	-0.0000837 /s
Bottom friction coefficient	0.0025
Gravitational acceleration	9.81 m/s
Undisturbed water level (wrt chart datum)	0.763 m
Minimum depth used in stress terms	0.5 m

3. RESULTS

Four model runs (A-D) are documented here, each using a different combination of wind stress magnitude and direction, as shown in Table 1.

TABLE 1. Summary of Model Runs and the Wind Stress Forcing Applied

Model Run	Wind Stress (Pa)	(deg)	Wind Speed (m/s)	Wind Direction
A	0.1	45	8.5	South-west
B	1.0	45	25.0	South-west
C	0.1	135	8.5	North-west
D	0.1	315	8.5	South-east

These combinations were chosen after an examination of surface wind speed and direction statistics for Albany airport over a nineteen year period (Bureau of Meteorology, unpublished data). These data indicate that moderate, prevailing winds are south-easterlies in summer, and north-westerlies (swinging to south-west) in winter. Average wind speed is around 7.5 m/s.

The strongest wind events (> 15 m/s) come from the south-west or the north-west, however these events occur for only a small percentage of the total time. According to convention, the direction ascribed to a wind stress vector is the direction to which the wind is travelling, whereas the direction of a wind velocity vector is that from which the wind is coming.

The results of the model runs are given in appendices A-D and are presented graphically in the following forms:

- time-series of elevation, depth-averaged current speed and direction, registered at specified locations (shown in Figure 3),
- steady-state water level contour maps,
- steady-state depth-averaged water current fields,
- fields of steady-state volume flux rates per unit width of water column.

Model runs were also made for west, east, north and south wind directions, but these results are not presented.

4. DISCUSSION OF RESULTS

Constant uniform winds were applied in order to isolate the basic response characteristics of PRH to local wind forcing. As far as possible, the results are discussed in a generalised sense, emphasising main features rather than the individual details of each model run.

4.1 Time-series of Surface Elevations and Current Velocities

The time-series results for elevations and currents at specified locations display several common features:

(a) immediately following the onset of the wind stress, water is accelerated in a downwind direction, regardless of its position in PRH. This occurs for a very short period before either bottom friction or pressure gradient forces (the latter due to surface slopes) have had time to grow. The initial momentum balance is simply between the wind stress and fluid inertia. This feature can be clearly seen in Figures D.1 and D.2.

(b) the onset of wind excites periodic oscillations which gradually decay under the influence of bottom friction. These oscillations, present in both the elevation and velocity response, represent water sloshing back and forth between boundaries of PRH in the form of standing waves (or seiches). For example, a wind stress to the south-east excites oscillations of period about 50 minutes. At opposite ends of PRH, water level fluctuations are large in amplitude and opposite in phase (Figure C.1.). Across the centre of PRH, the fluctuations exhibit low elevation amplitudes, but significant current amplitudes (Figure C.2). These features suggest that the dominant seiche occurs as a fundamental mode over the length (8.1 km) of PRH.

The period T of a fundamental seiche in a closed basin of uniform depth is given (e.g. Weigel, 1964) by

$$T = 2 L / \sqrt{(gh)}$$

where L is the basin length, h its depth, and g the gravitational acceleration. For dimensions representative of PRH (L=8.1 km, h=3.0 m) this simple formula yields a period in agreement with that predicted by model run C.

Winds from other directions may excite standing waves of different periods. Wind stress to the north-east produces oscillations of about 30 minutes period (Figures A.1 and A.4). In this case the seiching motion is determined by the width of PRH and areas of deeper water.

The magnitude of the wind stress does not alter the period of the standing wave but does affect the rate of its decay. The time scale for frictional decay of these oscillations is approximately 6 hours for a wind stress of 0.1 Pa and 2 hours for a stress of 1 Pa (e.g. compare Figures A.1 and B.1).

(c) underlying the standing waves described above is an almost step-like elevation response everywhere to the wind, i.e. the water surface first reaches the level of its steady-state elevation within a fraction of a standing wave period.

However the underlying depth-averaged current response varies as a function of local water depth, wind stress magnitude and wind stress direction. The current speed initially increases with time, until bottom friction becomes important. The current then tends to a steady-state speed and direction. The 'establishment times', defined here as the times taken to reach 0.5 of the steady-state current speeds, are shown in Table 2 for each of the model runs.

TABLE 2. 'Establishment Times' and Steady-state Current Speeds for model runs A-D

Site		Run A		Run B		Run C		Run D	
Grid Cell	Depth (m)	Speed (m/s)	Time (min)	Speed (m/s)	Time (min)	Speed (m/s)	Time (min)	Speed (m/s)	Time (min)
(6,24)	0.5	0.07	20	0.25	10	0.16	23	0.15	23
(7,4)	2.9	0.03	153	0.11	31	0.12	63	0.05	27
(4,12)	2.7	0.05	72	0.16	<40	0.10	72	0.12	83
(14,12)	11.8	0.07	288	0.16	54	0.10	315	0.08	221

Response is slower in deeper water for the same wind stress (e.g. Figures C.2 and D.2), and is more rapid under increased wind stress for the same water depth (compare Figures A.1 and B.1). Wind direction determines the number of circulatory gyres and their disposition with respect to the locations at which detailed time-series results are available. When one of these locations is near the common edge of two counter-rotating gyres, the response there may not be exponential, and the time to approach a steady-state vector may be long. This is the case for runs A and B at grid cell (14,12), as shown in Figures A.4 and B.2.

For wind stresses of 0.1 Pa, the establishment times range up to 5 hours, whereas steady-state currents are established in about 1 hour for gale force wind stresses of 1 Pa (see Figures A.4 and B.2). These results are broadly consistent with the frictional adjustment time scales which can be deduced (see Csanady, 1982) for flows governed by a simple balance between inertia, wind stress and bottom friction.

In response to the ten-fold increase in wind stress, the steady-state speeds are increased by a factor of about 3.

4.2 Water Level Distribution in the Steady-state.

The steady-state water surface contours are aligned almost perpendicular to the wind. The water surface is raised adjacent to downwind shores and depressed adjacent to upwind shores, so that the pressure gradient force is in opposition to the wind stress. Surface slopes tend to be greater in shallow areas, and smaller in deeper areas. For a north-east wind stress of 0.1 Pa the maximum water level differential over PRH is about 0.03 m (Figure A.7), while for a north-east wind stress of 1 Pa, the differential increases to about 0.3 m (Figure B.3). In the latter case there is an exposure of approximately 0.1 km^2 of the PRH bed at its western end, which occurs within 2 hours of the wind onset.

4.3 Current Velocity Distribution in the Steady-state

Depth-averaged current vector fields show that the steady-state water circulation consists of interacting gyres which are controlled by the wind stress magnitude and direction, and the form of the coastline and bathymetry. The juxtaposition in PRH of extensive, shallow, marginal banks, and a deeper basin is significant. Currents tend to be driven along isobaths, with a downwind component in shallow water areas, and with an upwind component in deeper water areas; currents tend to be stronger in shallow water or in areas of horizontal convergence (e.g. Figure D.4). This behaviour may be explained in two ways:

(a) a wind stress distributed uniformly over the entire water surface may be thought of as acting through the centroid of the surface areas. In a basin of non-uniform depth the line of action of the wind stress does not coincide with the centre of mass of the water body. Thus a torque is generated which induces water circulation, (Fischer et al, 1979), or alternatively,

(b) wind stress causes inclination of water surfaces near coasts. In shallow water the wind stress is greater than the total gravity force due to water surface slope, and the current is driven with a component in the downwind direction. In deeper water the gravity force dominates the wind stress, and water is driven upwind (Csanady, 1982).

Flow patterns are remarkably similar, regardless of wind speed, for winds of the same direction (e.g. Figures A.8 and B.4 for north-east stresses of 0.1 Pa and 1.0 Pa, respectively).

The wind direction determines whether there is one dominant sense of circulation (e.g. Figure D.4 for a south-east wind stress), or two major counter-rotating gyres (e.g. Figure A.8 for a north-east wind stress).

4.4 Volume Flow Rates

The distribution of steady-state depth-integrated volume flow rates per metre of water column width has been calculated for each model run (e.g. Figure A.9). Volume flow rates in a limited area of deep water near the port are much greater than elsewhere, and are able to balance the total flux over the rest of PRH.

5. GENERAL DISCUSSION

In this study, the influences of wind on external water levels and on flows through the harbour entrance have been neglected. These simplifications are not expected to significantly alter the wind-induced surface slopes in the steady-state. Thus the steady-state force balances and circulation patterns predicted by the model should be indicative of the steady-state responses to wind of PRH. However the times to establish these circulation patterns may be controlled by the rate of response to wind of waters outside the harbour.

No attempt has been made at this stage to calibrate the model by comparing its performance with field observations. Hence the model results should be considered only as indicative of the general nature of the wind-driven circulation. Calibration would principally involve adjustments to the parameter values in the bottom stress terms and would need to take into account factors such as the distribution of sea bed vegetation (and its effects on bottom roughness) and the influence of motions not directly included in the hydrodynamic model (e.g. wave motions). Comparison with field data will be deferred until the model is adapted to run with an 'open', seaward boundary condition, and until observed tidal and wind effects are modelled together.

6. IMPLICATIONS

This study has shown that local wind stresses can generate currents of considerable importance in PRH. Over a wide range of wind strengths, depth-averaged currents of about 1-2% of the wind speed may be attained (e.g. Table 2).

For winds of a given direction and duration, the excursion of the water increases more than proportionally with the wind speed since, not only do the steady-state velocities increase, but the steady-state 'establishment times' are reduced. A wind of 0.1 Pa must act for 4-5 hours in a given direction to generate near steady-state currents, whereas a wind of 1 Pa needs to act only for 1-2 hours.

West to north winds generate predominantly anti-clockwise circulation. East to south winds generate predominantly clockwise circulation. Steady winds within these direction ranges drive one major gyre which covers most of the area of PRH. For winds swinging within these direction ranges, water movements will generally be consistent and cumulative. For winds swinging into or out of these ranges, current directions may be reversed and nett circulation limited. Minor gyres are of importance in conditions where stable wind directions are maintained over relatively long time scales. In these conditions, transport of effluent from within the area covered by the smaller gyres is likely to be slow. However, in conditions of rapid wind variation, minor gyres are likely to appear and disappear as wind direction changes.

Under south-west winds two major gyres are established and water exchange between different parts of PRH due to wind forcing may be more limited than is the case for winds from other directions at the same wind speed.

The western shallow shelf, on parts of which pollution problems have been encountered, has a length of about 3 km. Moderate winds (0.1 Pa) must be maintained for at least 6 hours (north-west wind) and up to 12 hours (south-west wind) to produce water excursions of this length.

Compared with other wind directions, south-westerlies are not efficient agents of flushing on the western shallows, which are oriented almost perpendicular to this wind direction. A wind stress of 1 Pa to the north-east (south-west wind of 25 m/s), is scarcely more effective than a wind stress of 0.1 Pa to the north-west (south-east wind of 8.5 m/s).

For a wide range of unstratified environmental flows, vertical mixing of passive contaminant is achieved within a downstream distance of about one hundred times the flow depth (Hunter, per comm). Assuming this to be the case for the deep portions of PRH, a point discharge of contaminant will be vertically well-mixed within a distance of 1 200 m (four grid lengths).

Volume flow rates are generally greater in areas of deep water than in shallow water areas. Therefore, an effluent continuously discharged to deep water, and rapidly mixed through the water column, will undergo greater dilution than would be the case for an equivalent discharge to shallow water. However, the overall water exchange rate between PRH and King George Sound should be quantified in order to fully assess the impacts of effluent discharges to the harbour.

7. ACKNOWLEDGEMENTS

Mr D Pitt constructed the computer plotting routines. Dr J Hunter read the manuscript and provided valuable comments and suggestions. Dr J Ottaway contributed editorial and technical assistance.

8. REFERENCES

Atkins R.P., Iveson J.B., Field R.A. & Parker I.N. (1980) A technical report on the water quality of Princess Royal Harbour, Albany. Bulletin no. 74, Department of Conservation and Environment.

Courant R., Friedrichs K. & Lewy H. (1928) Uber die partiellen Differenzengleichungen der mathematishchen. Phys. Math. Ann., 100, 32-74.

Csanady G.T. (1982) 'Circulation in the coastal ocean.' pp 174-76 (D. Riedel: Dordrecht).

Fischer H.B., List E.J., Koh R.C.Y., Imberger J. & Brooks N.H. (1979) 'Mixing in inland and coastal waters' pp 232-234 (Academic Press: New York).

Flather R.A. & Heaps N.S. (1975) Tidal computations for Morecambe Bay. Geophys. J.R. Soc. 42, 489-517.

Hodgkin E.P. & Di Lollo V. (1958) The tides of south-western Australia. J. Roy. Soc. of W.A., 4(2), 42-54.

Hunter J.R. (1983) Numerical simulation of currents in Koombana Bay and the influence of the proposed new power station. Environmental Dynamics Report Number ED 83-049, Department of Civil Engineering, University of Western Australia.

Jackson M., Gorman R., Hancock D., Chittleborough G. & Talbot V. (1984) Mercury contamination in Princess Royal Harbour, Albany. Report of the ad hoc working group established by the Department of Public Health, Environmental Note No. 155, Department of Conservation and Environment, Western Australia.

Mills D.A. (1985) A numerical hydrodynamic model applied to tidal dynamics in the Dampier Archipelago. Bulletin no. 190, Department of Conservation and Environment, Western Australia.

Talbot V. (1983) Lead and other trace metals in the sediments and selected biota of Princess Royal Harbour, Albany, Western Australia. Environmental Pollution (Series B) 5, 35-49.

Wiegel R.L. (1964) "Oceanographic engineering' pp 115-116 (Prentice-Hall: Englewood Cliffs, N.J.).

APPENDIX A

Model Run A - Response to a Wind Stress of 0.1 Pa to the North-east

Model run A computed the response of PRH to a wind stress of 0.1 Pa to the north-east (equivalent to a wind speed of 8.5 m/s from the south-west).

Surface elevation and depth-averaged current speed and direction time-series, covering the first 72 hours after the onset of the wind, are shown for grid cells (6,24) and (7,4) (Figures A.1 to A.3), and for grid cells (14,12) and (4,12) (Figures A.4 to A.6). These figures show oscillations of approximately 30 minutes period which decay during the first 6 hours. The most interesting feature of these results is the very long period required for the current speed at grid cell (14,12) to converge to its steady-state value, and the highly non exponential behaviour exhibited in the process of convergence. This behaviour is possibly related to the dynamic interaction of the two counter-rotating gyres formed under these wind conditions, since grid cell (14,12) lies close to the common periphery of these gyres.

Figure A.7 shows a contour plot of the water level distribution at a time 72 hours after the onset of the wind. The contours show that water level increases across the harbour in the downwind direction. The water surface slope is greater in the area over the western shallows, and smaller over the deeper basin of PRH. The maximum water level differential across the harbour is 0.03 m.

Figure A.8 shows the depth-averaged current velocity field after 72 hours. The water circulates via two main gyres. The larger gyre, covering the entire south-eastern portion of the harbour, circulates in an anti-clockwise direction. Relatively high velocities (up to 0.14 m/s) are induced in the downwind direction across the south-eastern shallows, with low velocities occuring in the upwind direction in the middle of the harbour. The other major gyre, situated to the north-west has clockwise circulation.

Figure A.9 shows volume flow rates through the harbour. The main features of volume transport are similar to those of the velocity vector field, i.e. two gyres are set up, with opposite circulations. However, volume flow rates are large in deep areas and small in shallow areas.

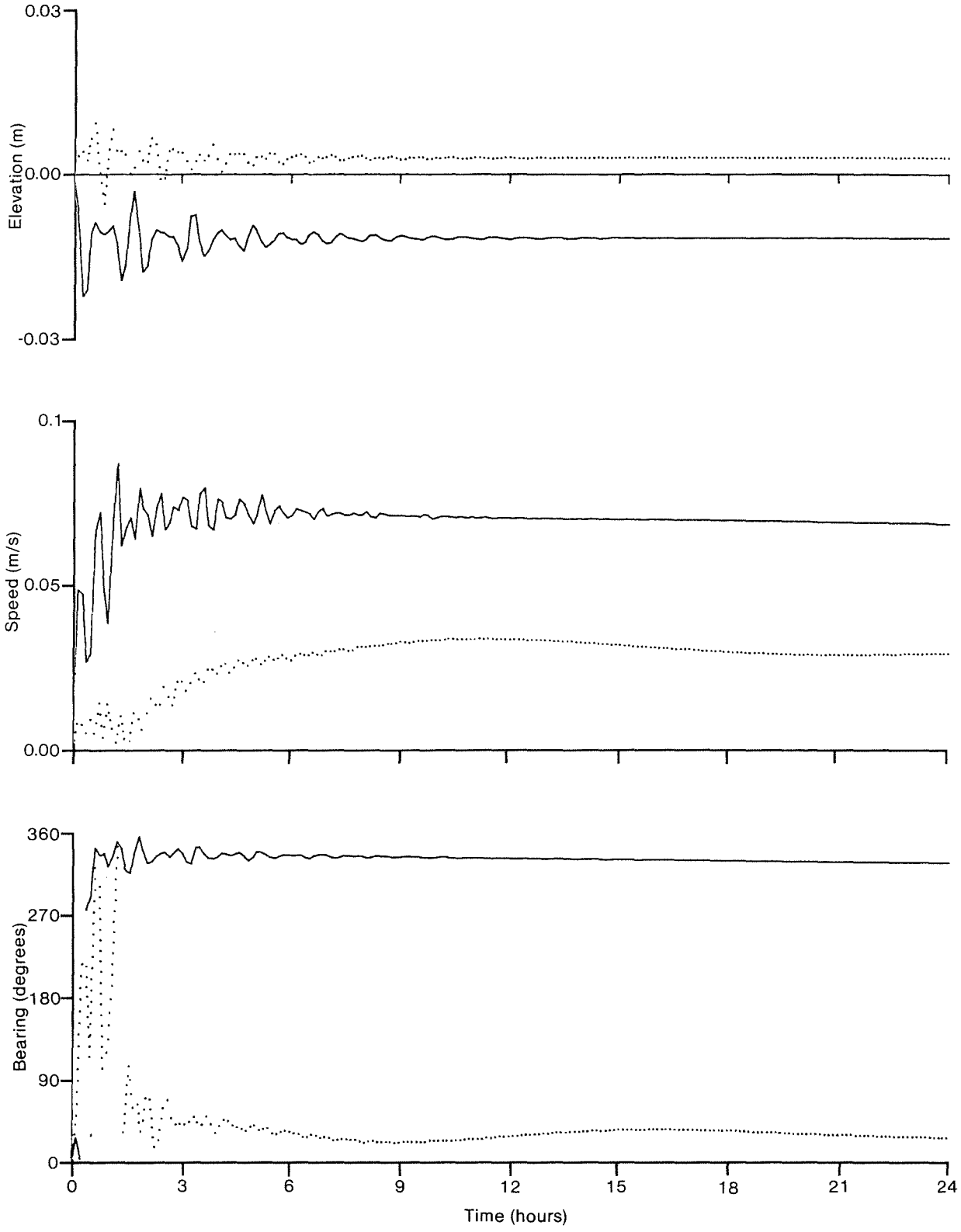

Figure A.1: Time-series of elevation, current speed and direction at cell 6,24 (————) and cell 7,4 (·····), 0-24 hours after the onset of a 0.1 Pa wind stress to the north-east.

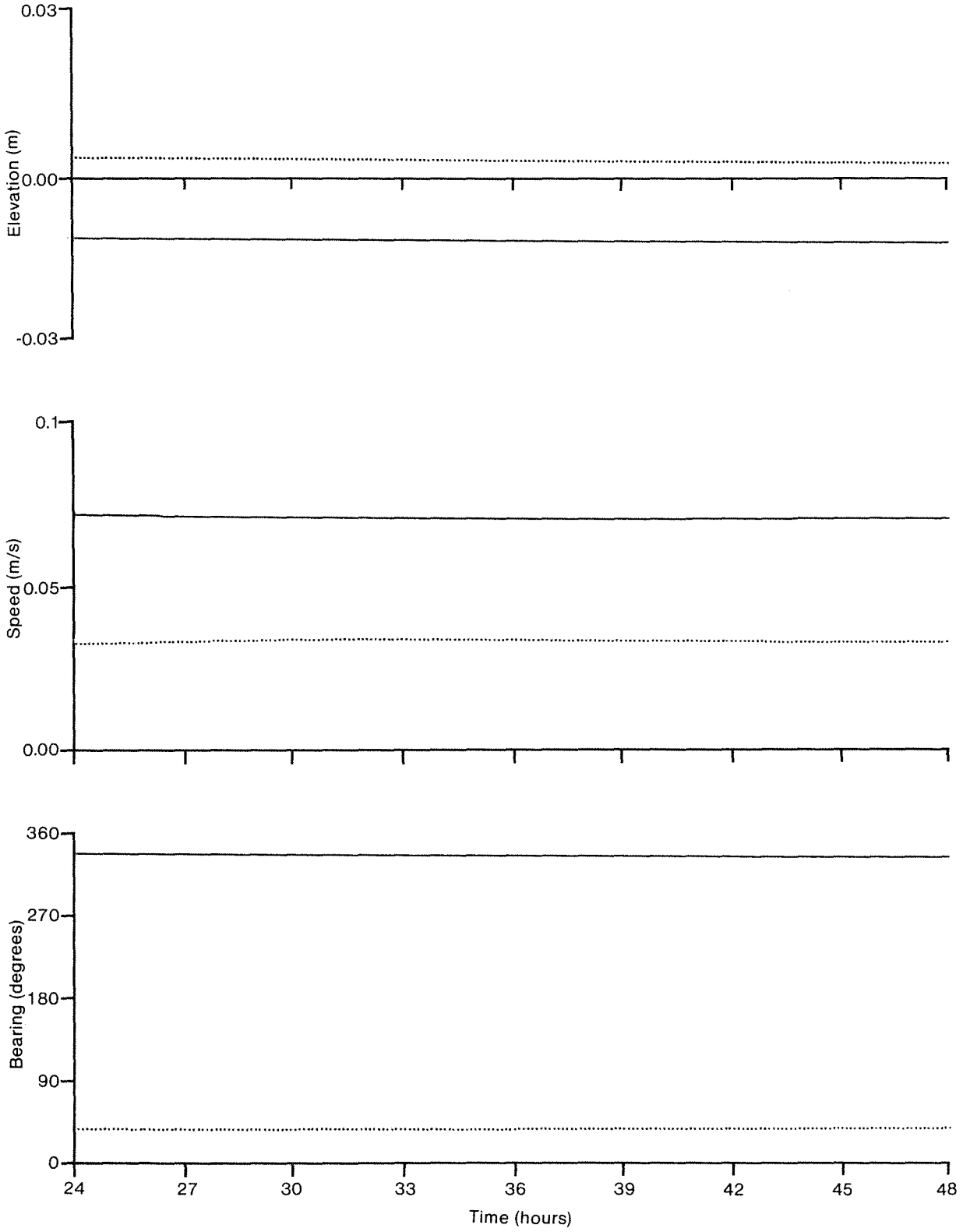

Figure A.2: Time-series of elevation, current speed and direction at cell 6,24 (————) and cell 7,4 (·····), 24-48 hours after the onset of a 0.1 Pa wind stress to the north-east.

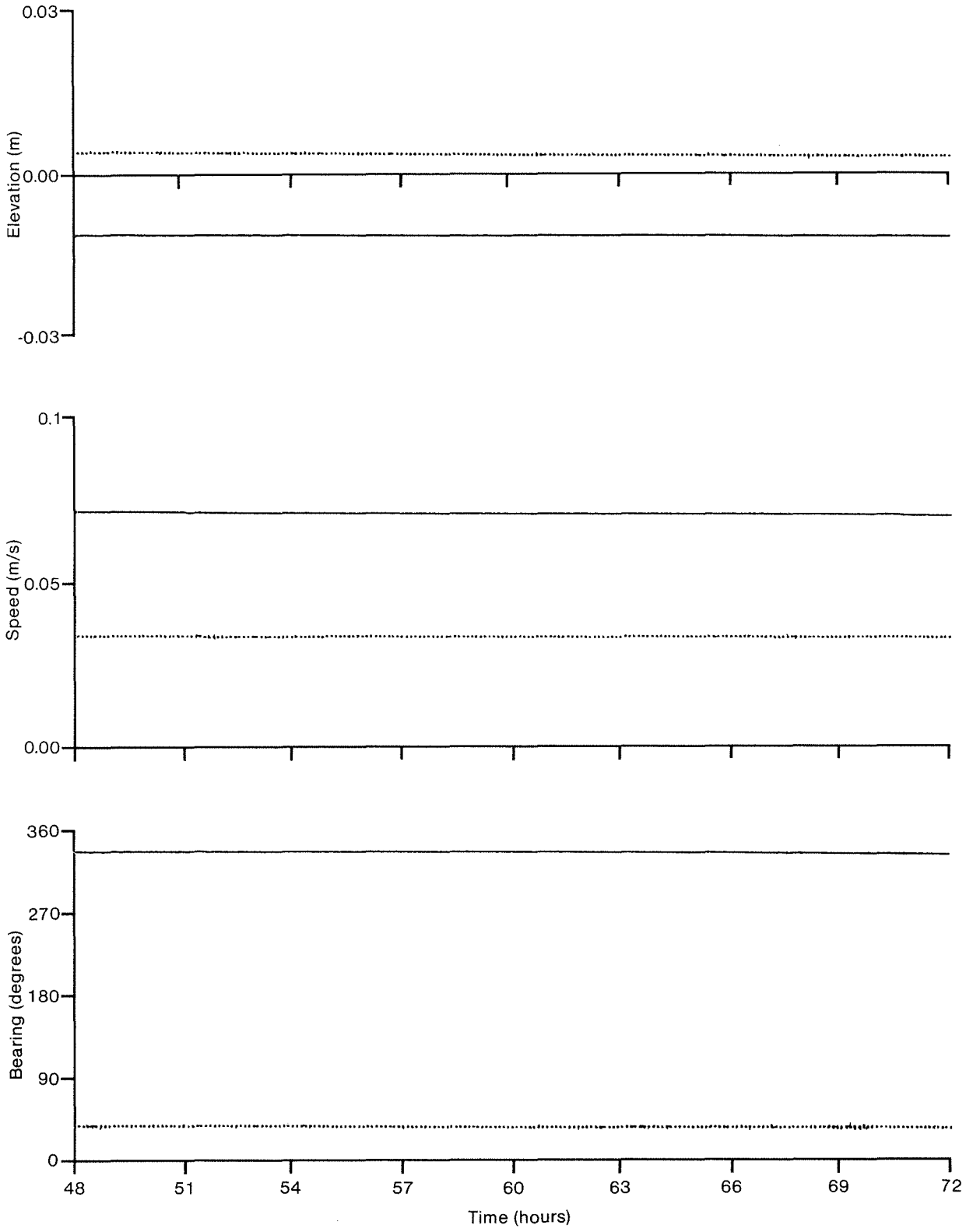

Figure A.3: Time-series of elevation, current speed and direction at cell 6,24 (————) and cell 7,4 (·····), 48-72 hours after the onset of a 0.1 Pa wind stress to the north-east.

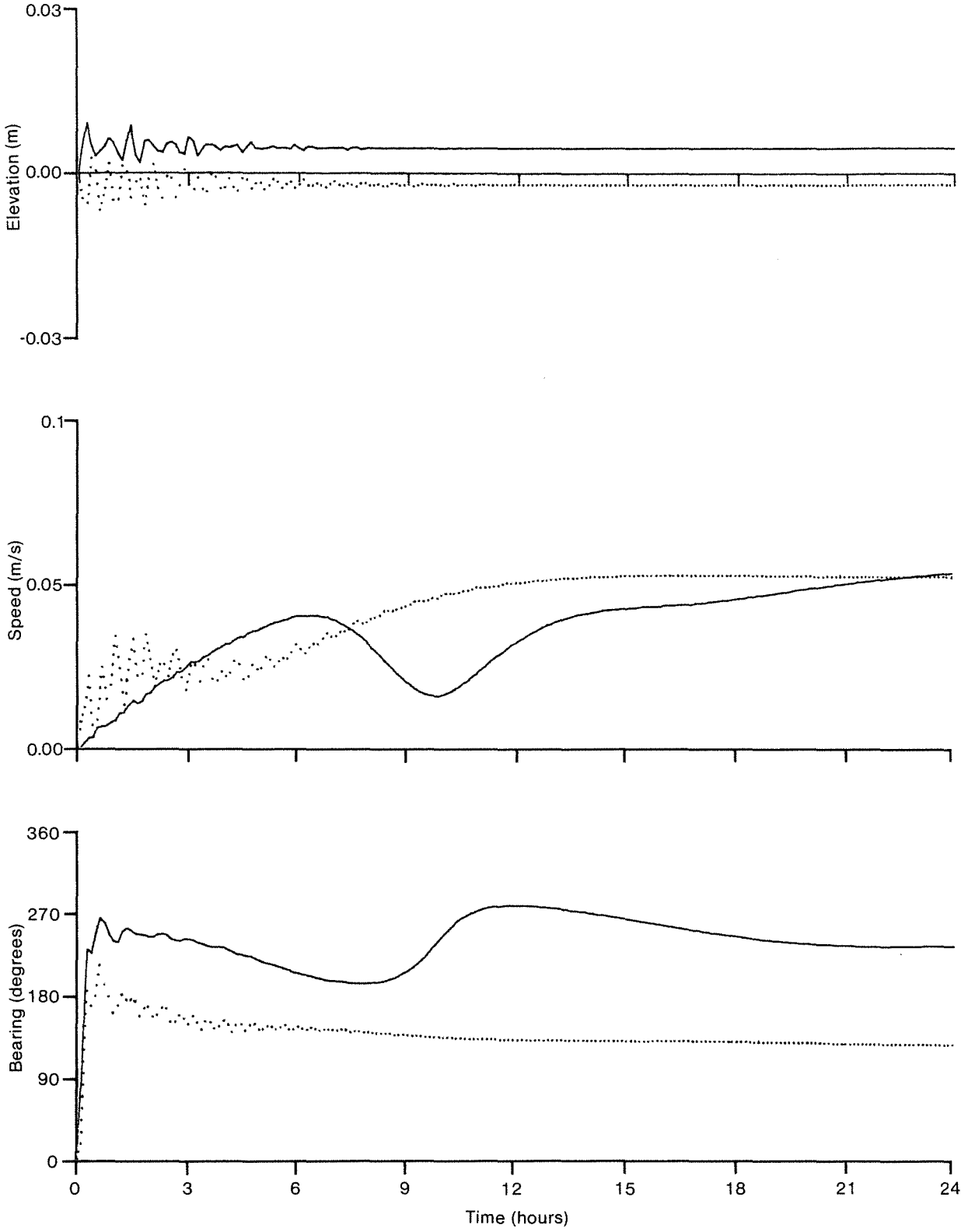

Figure A.4: Time-series of elevation, current speed and direction at cell 14,12 (————) and cell 4,12 (·····), 0-24 hours after the onset of a 0.1 Pa wind stress to the north-east.

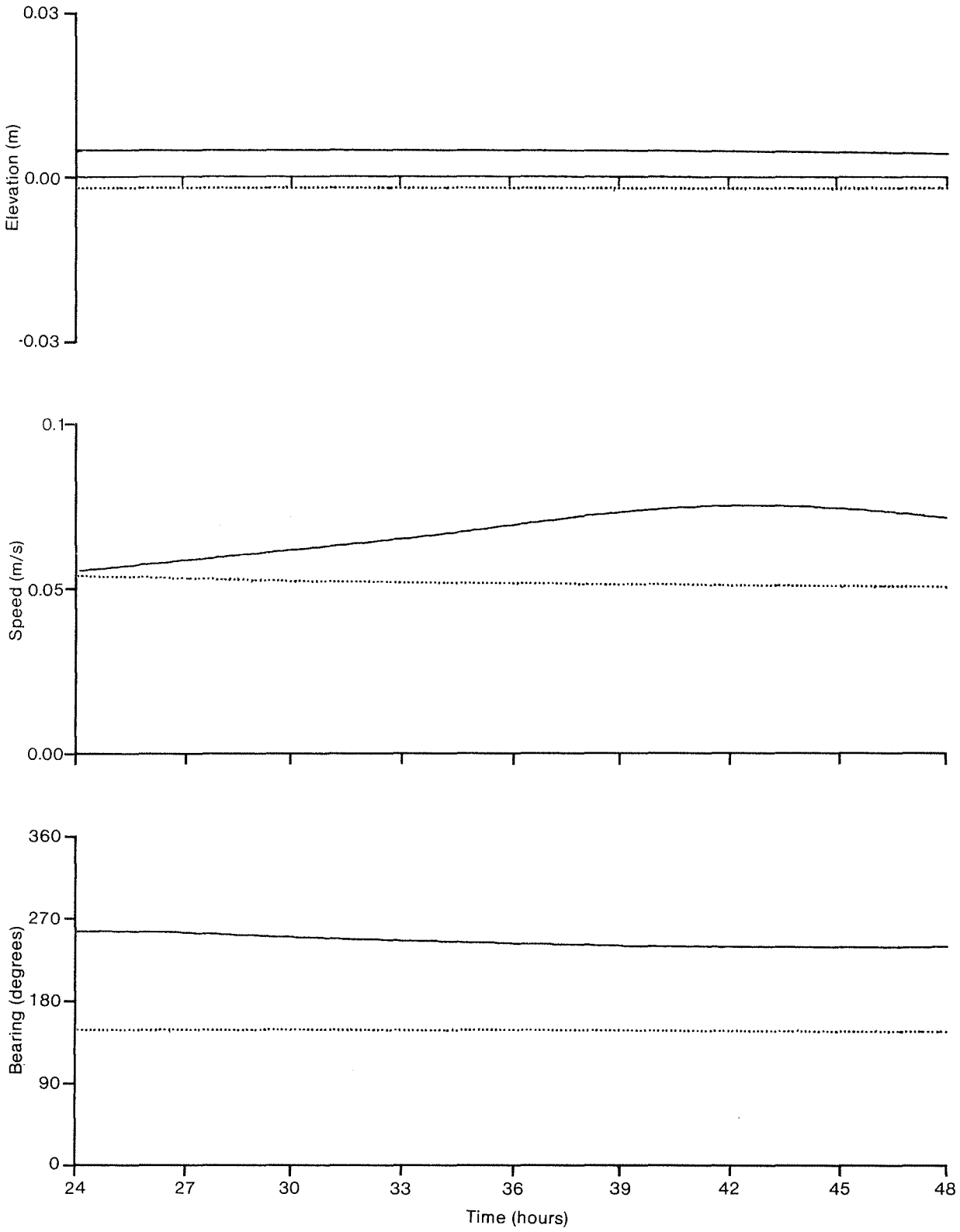

Figure A.5: Time-series of elevation, current speed and direction at cell 14,12 (————) and cell 4,12 (·····), 24-48 hours after the onset of a 0.1 Pa wind stress to the north-east.

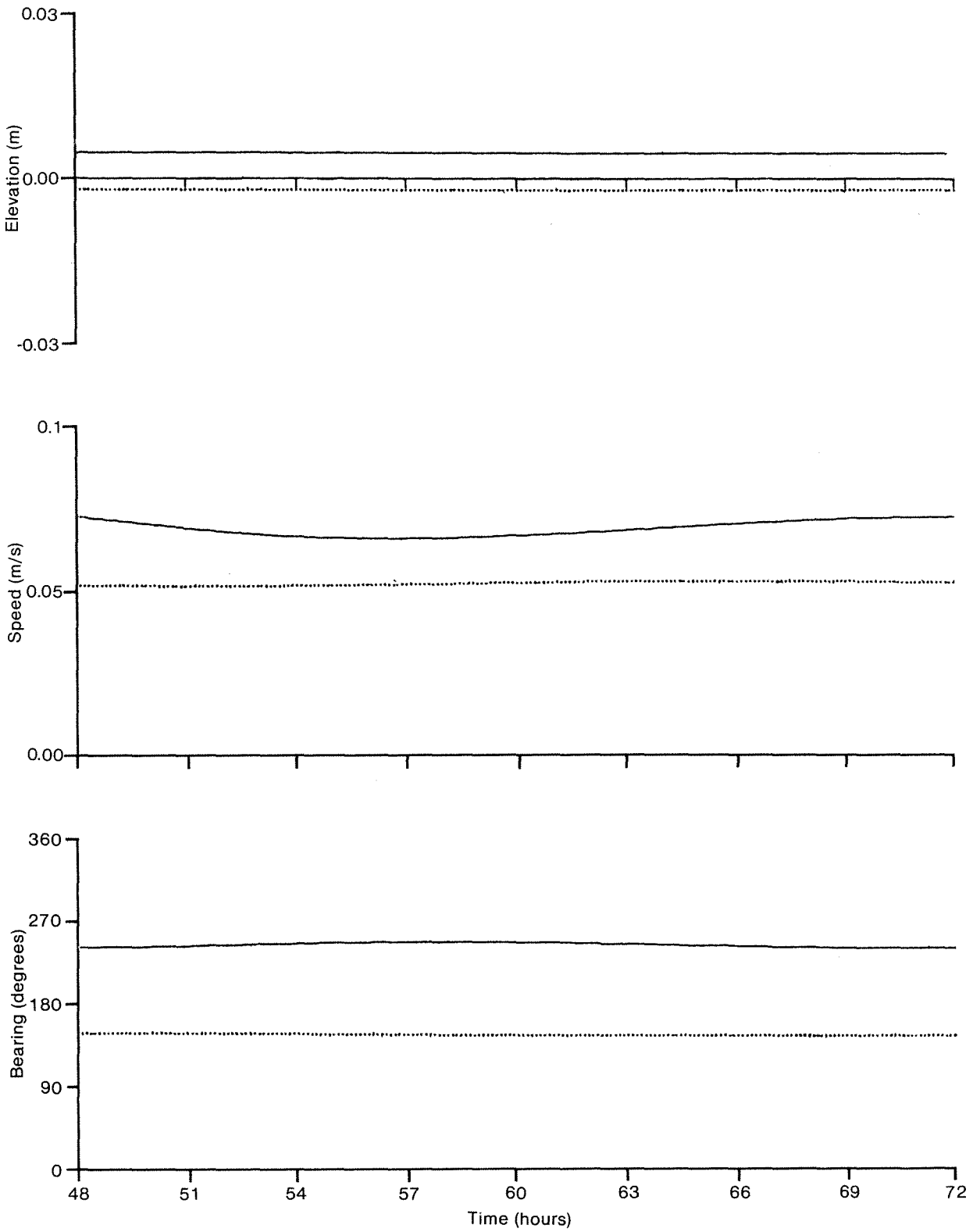

Figure A.6: Time-series of elevation, current speed and direction at cell 14,12 (———) and cell 4,12 (·····), 48-72 hours after the onset of a 0.1 Pa wind stress to the north-east.

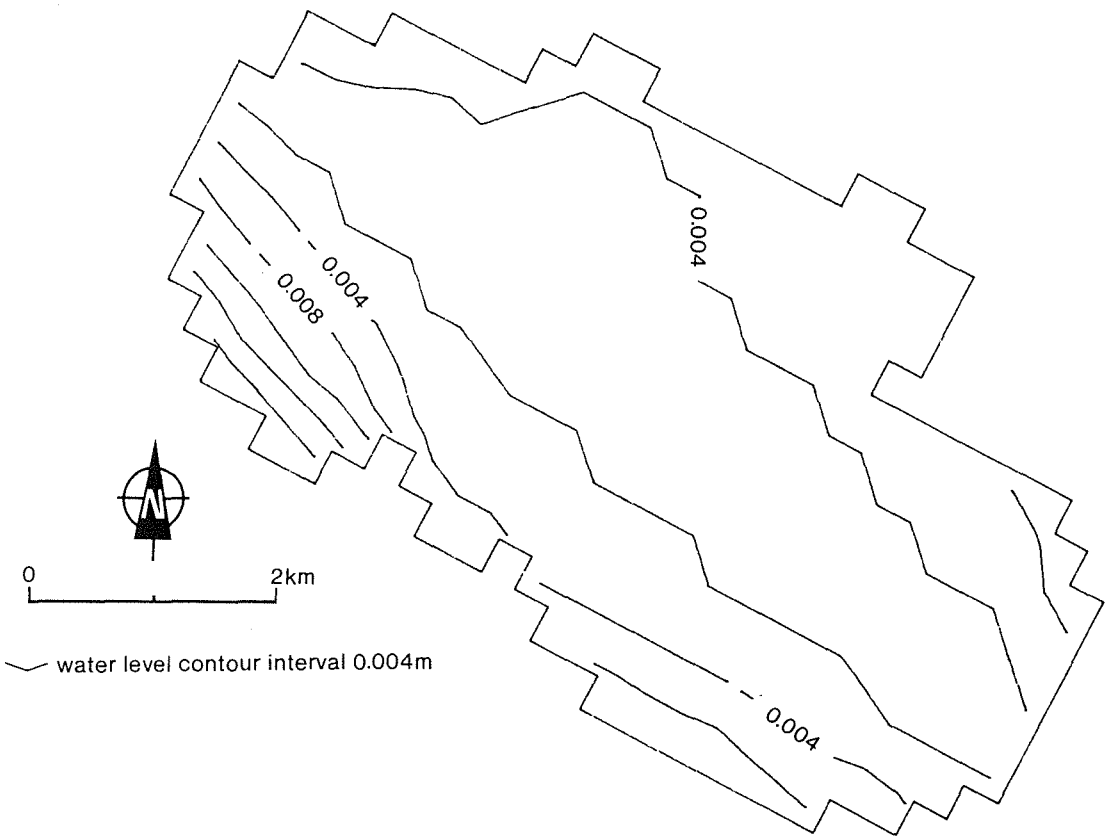

Figure A.7: Water level contours for a wind stress of 0.1 Pa to the north-east, 72 hours after onset of the wind.

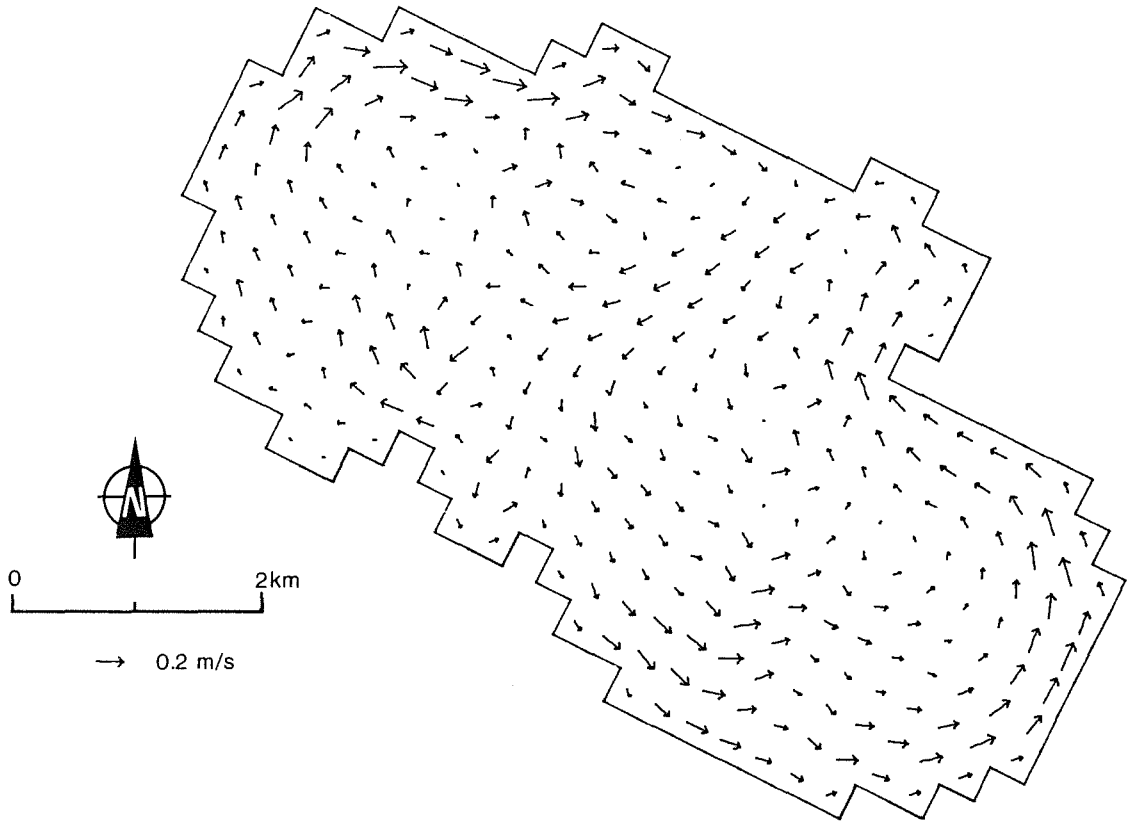

Figure A.8: Depth-averaged current velocity field for a wind stress of 0.1 Pa to the north-east, 72 hours after onset of the wind.

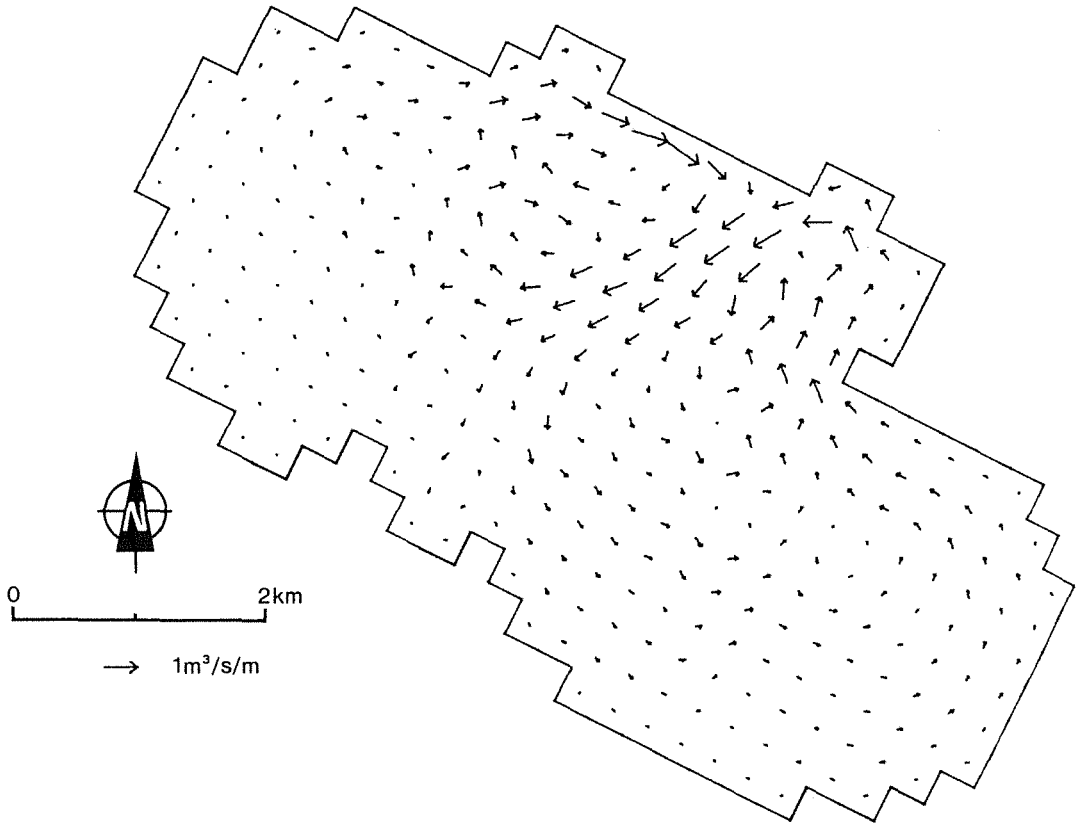

Figure A.9: Volume flow rate field for a wind stress of 0.1 Pa to the north-east, 72 hours after onset of the wind.

APPENDIX B

Model run B - Response to a Wind Stress of 1 Pa to the North-east

Model run B computed the response of PRH to a wind stress of 1.0 Pa to the north-east (equivalent to a wind speed of 25.0 m/s from the south-west). The wind stress direction is the same as for model run A, however its magnitude is ten times larger.

Time-series plots of surface elevation and water currents for the first 24 hours after onset of the wind are shown in Figures B.1 and B.2. Transient oscillations with periods of about 30 minutes, similar to those of run A, are generated, but decay within 2 hours. These oscillations are determined by the width of the harbour and the basin depth. Oscillations of 50 minutes period are also evident, suggesting that seiching also takes place along the length of the harbour. The low frequency water current response is highly non exponential at grid cell (14,12). This behaviour is probably related to the evolution of the two main counter-rotating gyres formed under the influence of south-west winds. In response to the higher value of wind stress applied for this model run, the establishment of steady-state currents occurs more rapidly, and the steady-state current speeds achieved are higher (by a factor of 3) than their counterparts in model run A.

Figure B.3 shows a contour plot of the water surface level at a time 24 hours after the onset of the wind. Water surface slope is greater by an order of magnitude, when compared with run A and the gradient is again largest in the area over the south-west shallows. The maximum water level differential across the harbour is 0.32 m, and an area of approximately 0.1 km^2 of the western shallows is exposed.

Figure B.4 shows the depth-averaged current velocity field after 24 hours. Velocities are higher than in model run A, reflecting the greater wind stress applied. Speeds of up to 0.5 m/s are generated in shallow water. The circulation pattern is generally similar to that of model run A.

Figure B.5 shows the corresponding volume flow rates through the harbour.

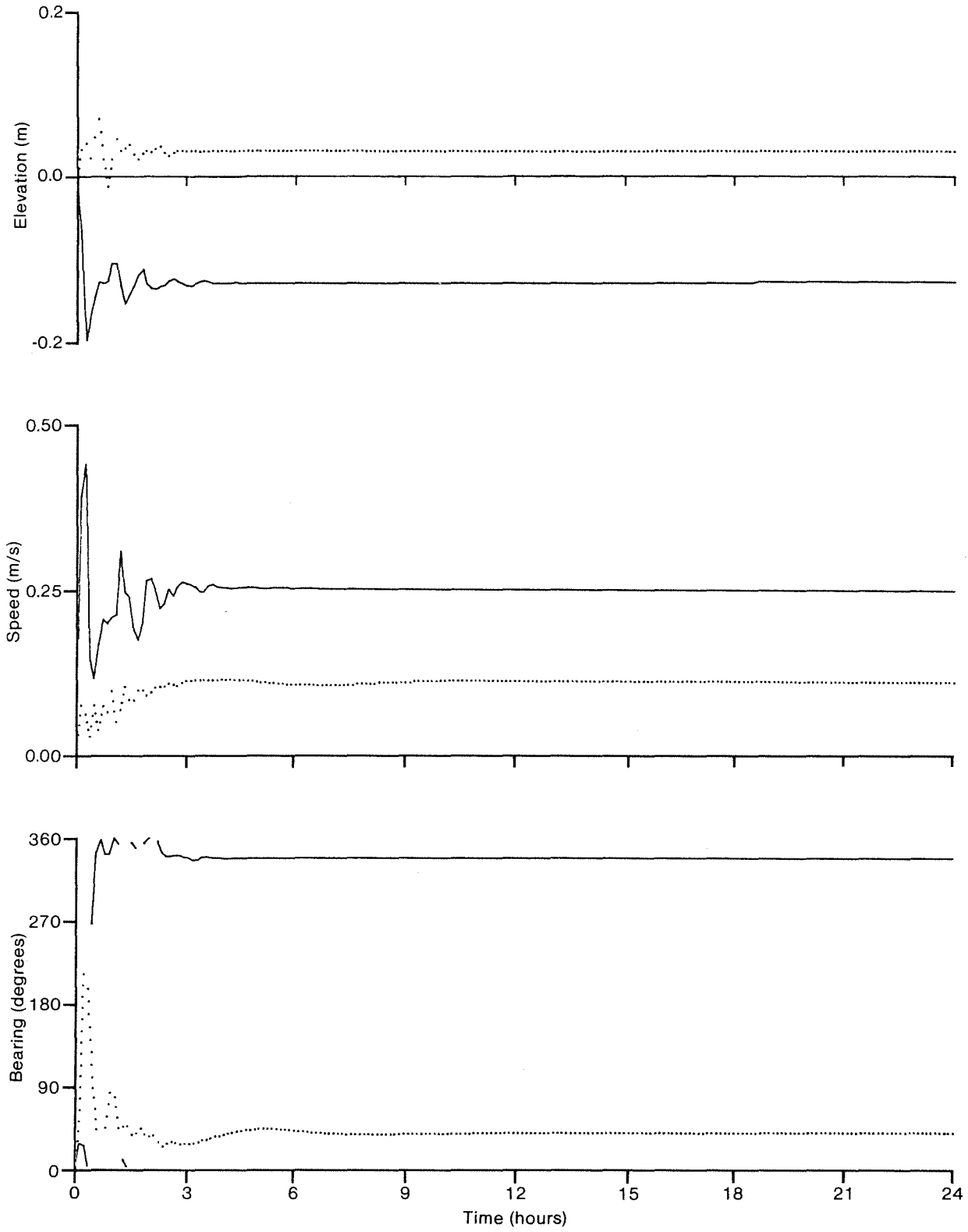

Figure B.1: Time-series of elevation, current speed and direction at cell 6,24 (————) and cell 7,4 (·····), 0-24 hours after the onset of a 1 Pa wind stress to the north-east.

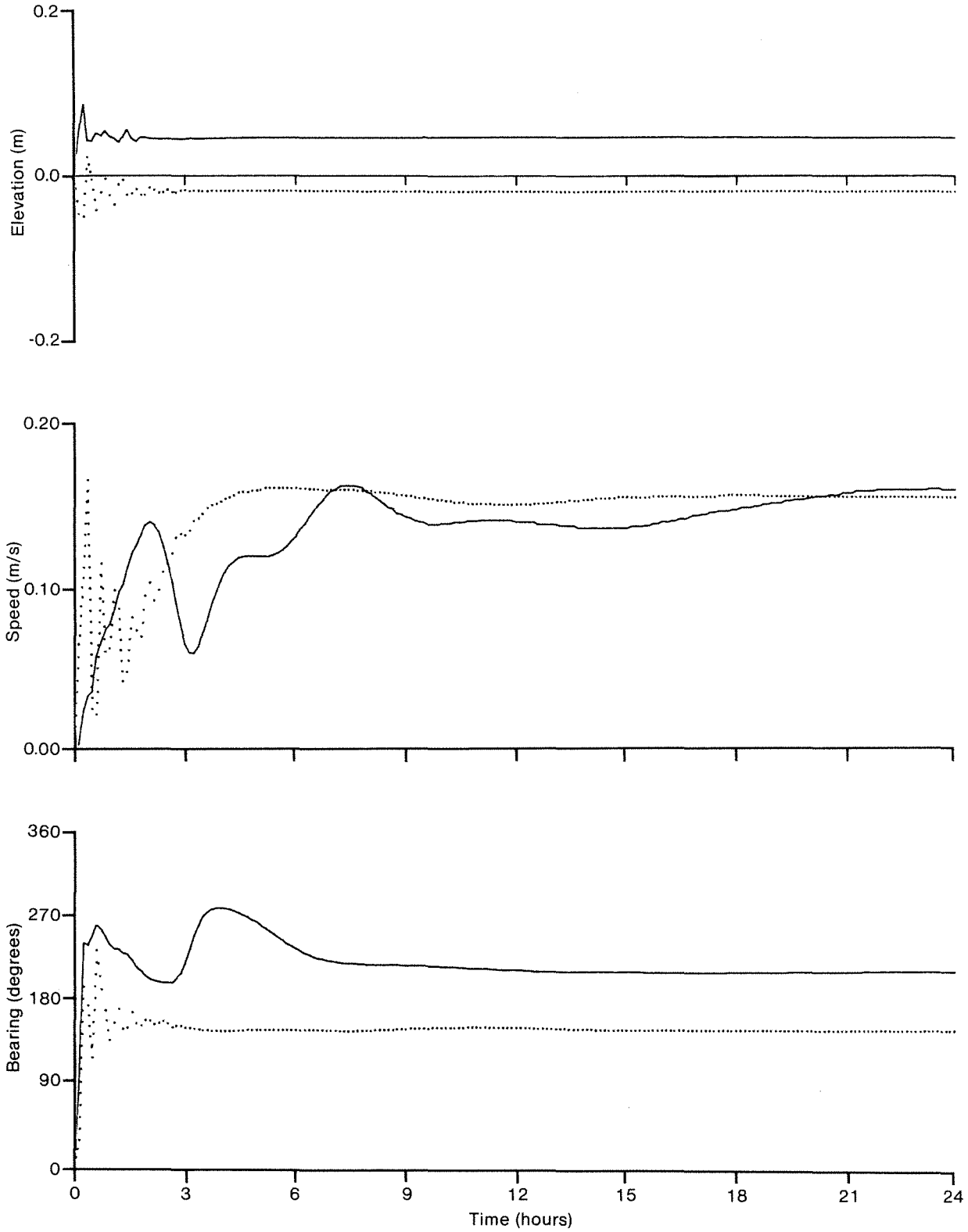

Figure B.2: Time-series of elevation, current speed and direction at cell 14,12 (————) and cell 4,12 (·····), 0-24 hours after the onset of a 1 Pa wind stress to the north-east.

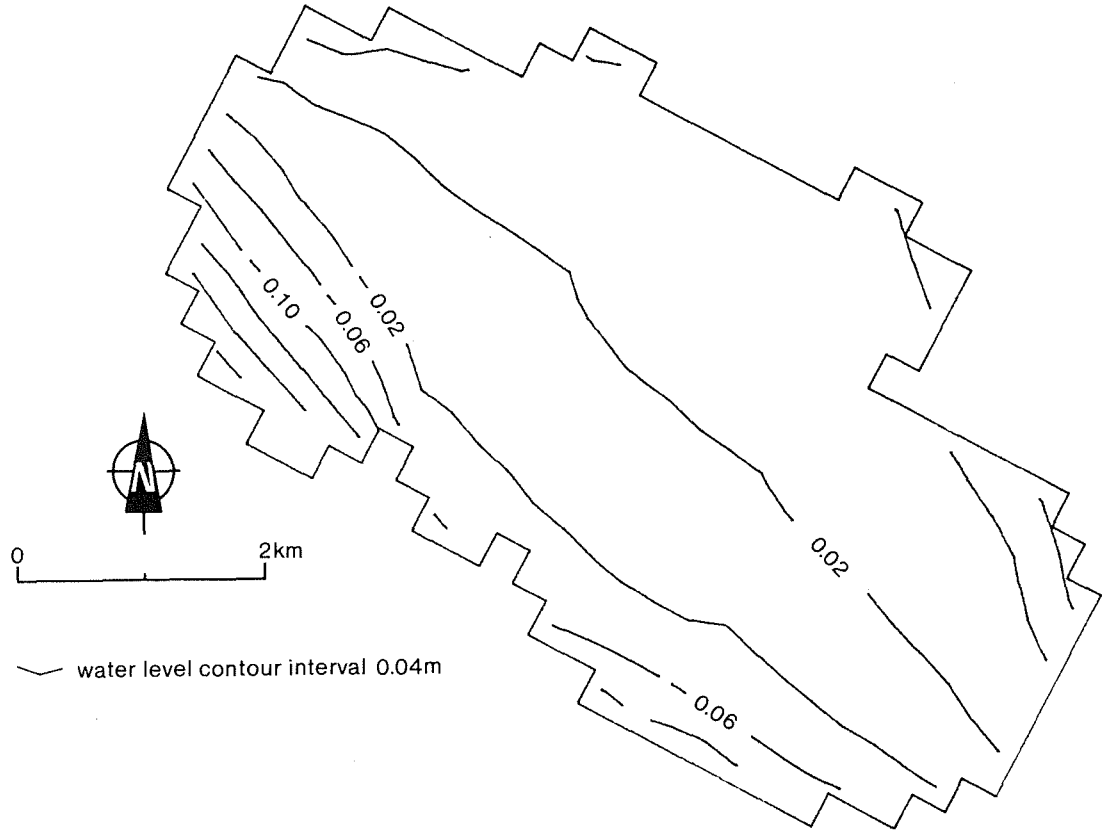

Figure B.3: Water level contours for a wind stress of 1 Pa to the north-east, 24 hours after onset of the wind.

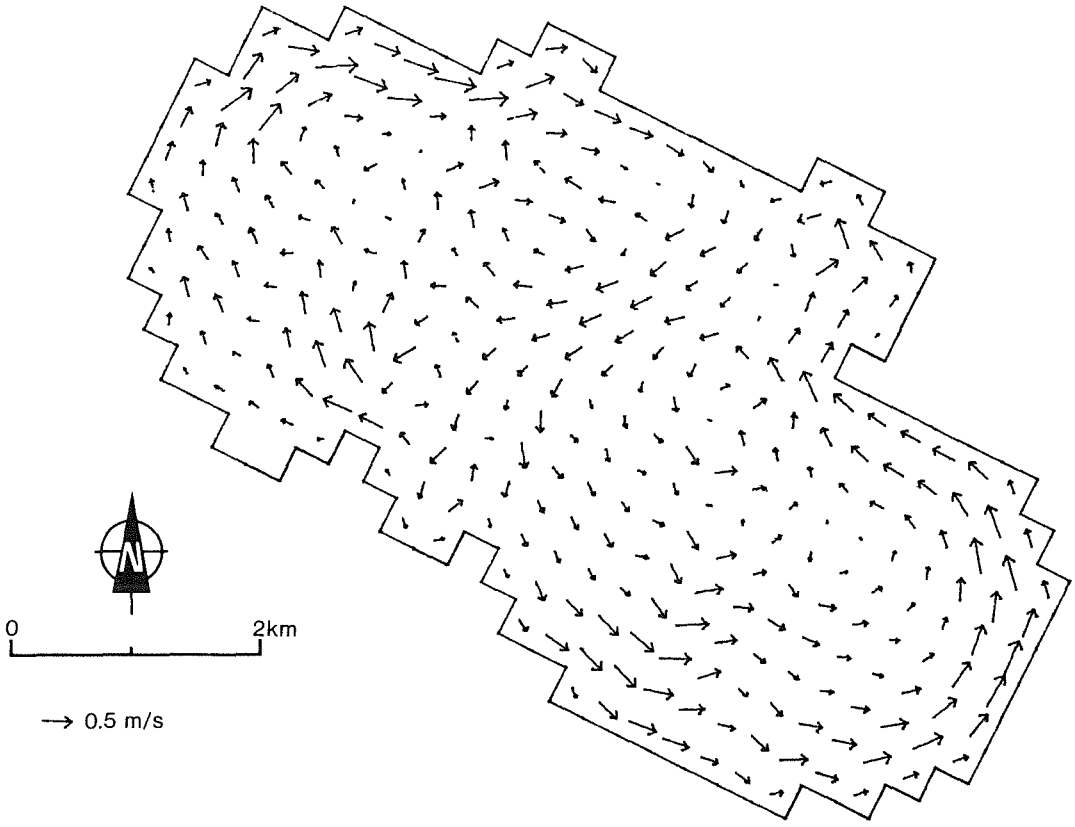

Figure B.4: Depth-averaged current velocity field for a wind stress of 1 Pa to the north-east, 24 hours after onset of the wind.

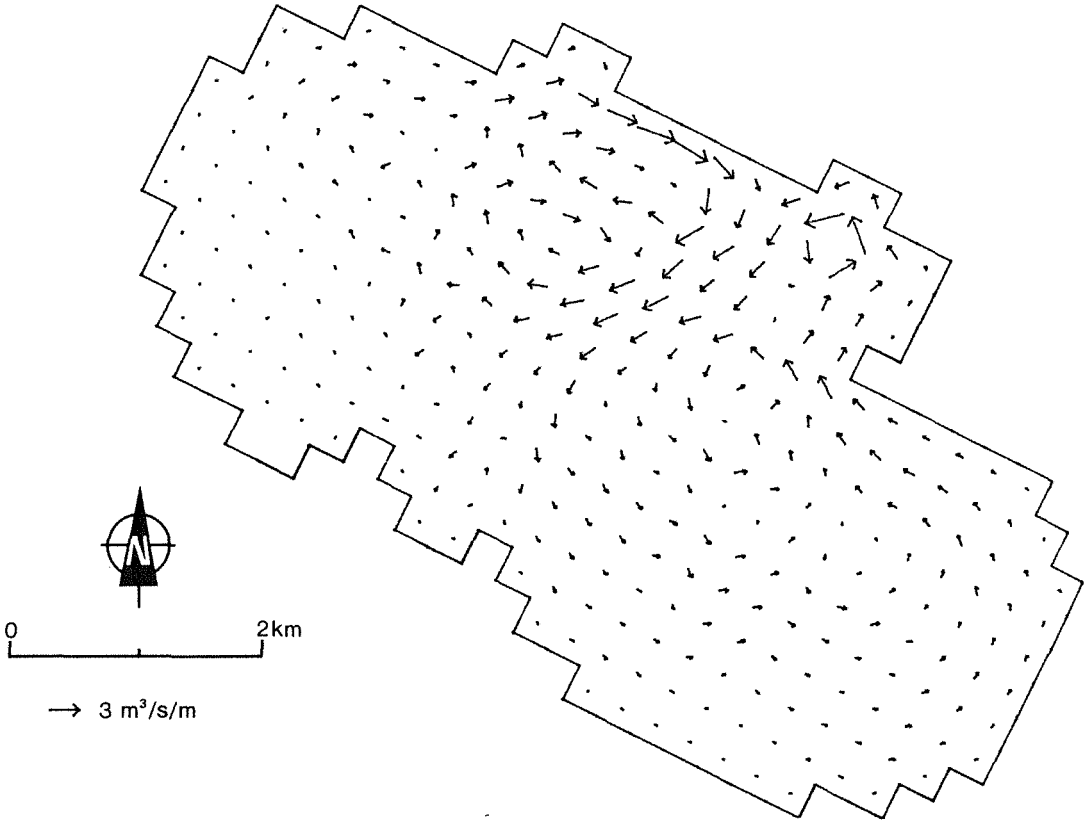

Figure B.5: Volume flow rate field for a wind stress of 1 Pa to the north-east, 24 hours after onset of the wind.

APPENDIX C

Model run C - Response to a Wind Stress of 0.1 Pa to the South-east

Model run C examined the response of PRH to a wind stress of 0.1 Pa in a south-easterly direction (corresponding to a wind speed of 8.5 m/s from the north-west).

Time-series plots of surface elevations and water currents for the first 24 hours after onset of the wind are shown in Figures C.1 and C.2. The dominant seiching activity is along the length of PRH with a period of approximately 50 minutes. Elevations at the north-west and south-east ends of the harbour are opposite in phase and large in amplitude (Figure C.1).

The low-frequency response of the currents shows an approximately exponential variation at all four grid cells for which time-series data are available. Establishment times for currents in the deepest areas are about 5 hours (Figure C.2).

A contour plot of the water surface level is shown in Figure C.3 for a time 24 hours after the onset of the wind. Water level contours align perpendicular to the wind direction. As in runs A and B, water level gradient is greater over the shallow margins than over the deeper basin of the harbour. Maximum water level differential is 0.036 m.

The depth-averaged current velocity field shown in Figure C.4, consists mainly of a large anti-clockwise gyre dominating water circulation in the harbour. Water moves in the downwind direction with speeds up to 0.2 m/s in shallow areas, whereas in deeper areas water moves more slowly in an upwind direction or perpendicular to the wind direction. Smaller gyres are established in the north-western and south-eastern parts of the harbour.

Figure C.5 shows that the largest volume flow rates occur in the dredged port area, smaller volume flow rates occur in the main basin of the harbour, and volume transports are smallest around the shallow margins.

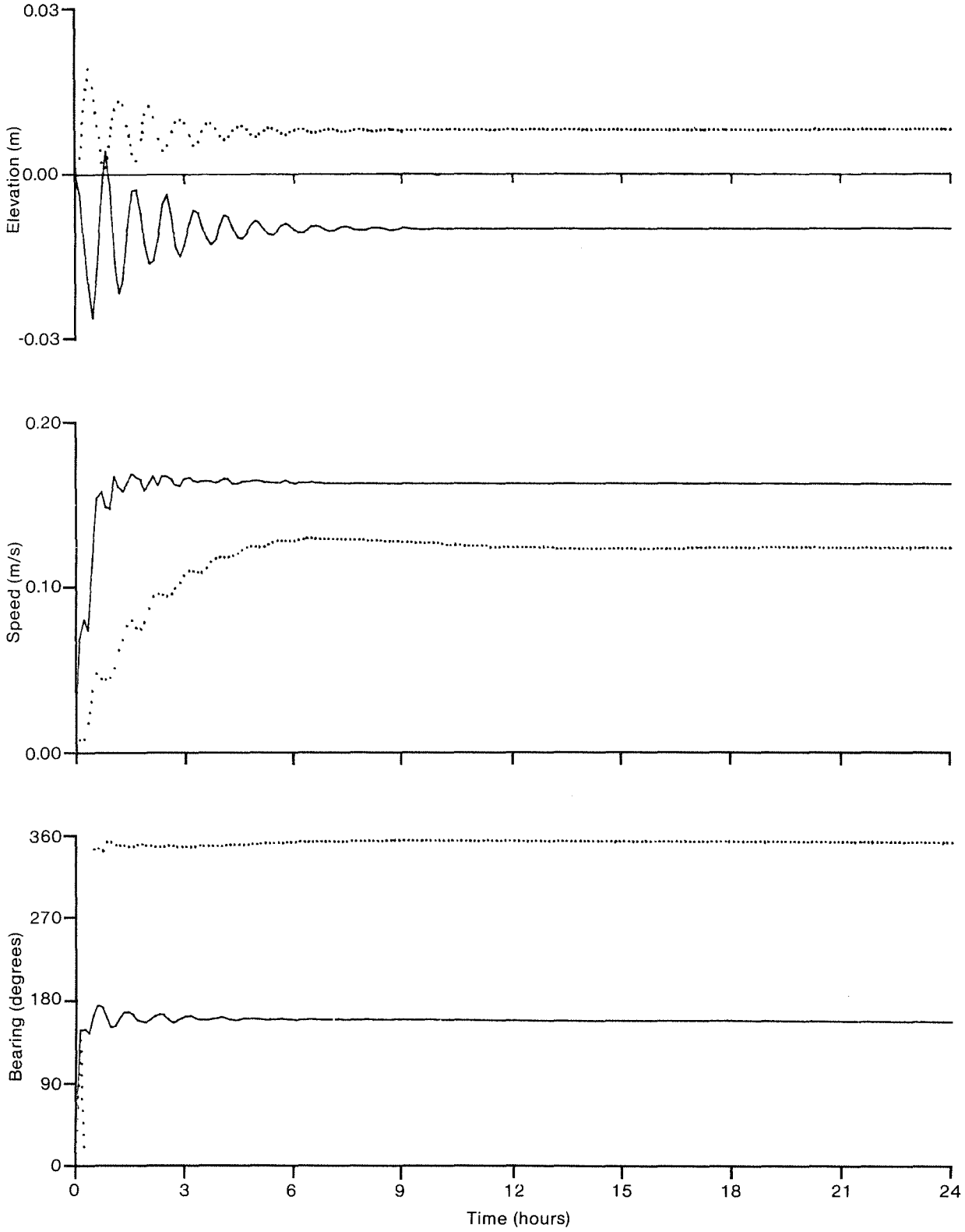

Figure C.1: Time-series of elevation, current speed and direction at cell 6,24 (————) and cell 7,4 (·····), 0-24 hours after the onset of a 0.1 Pa wind stress to the south-east.

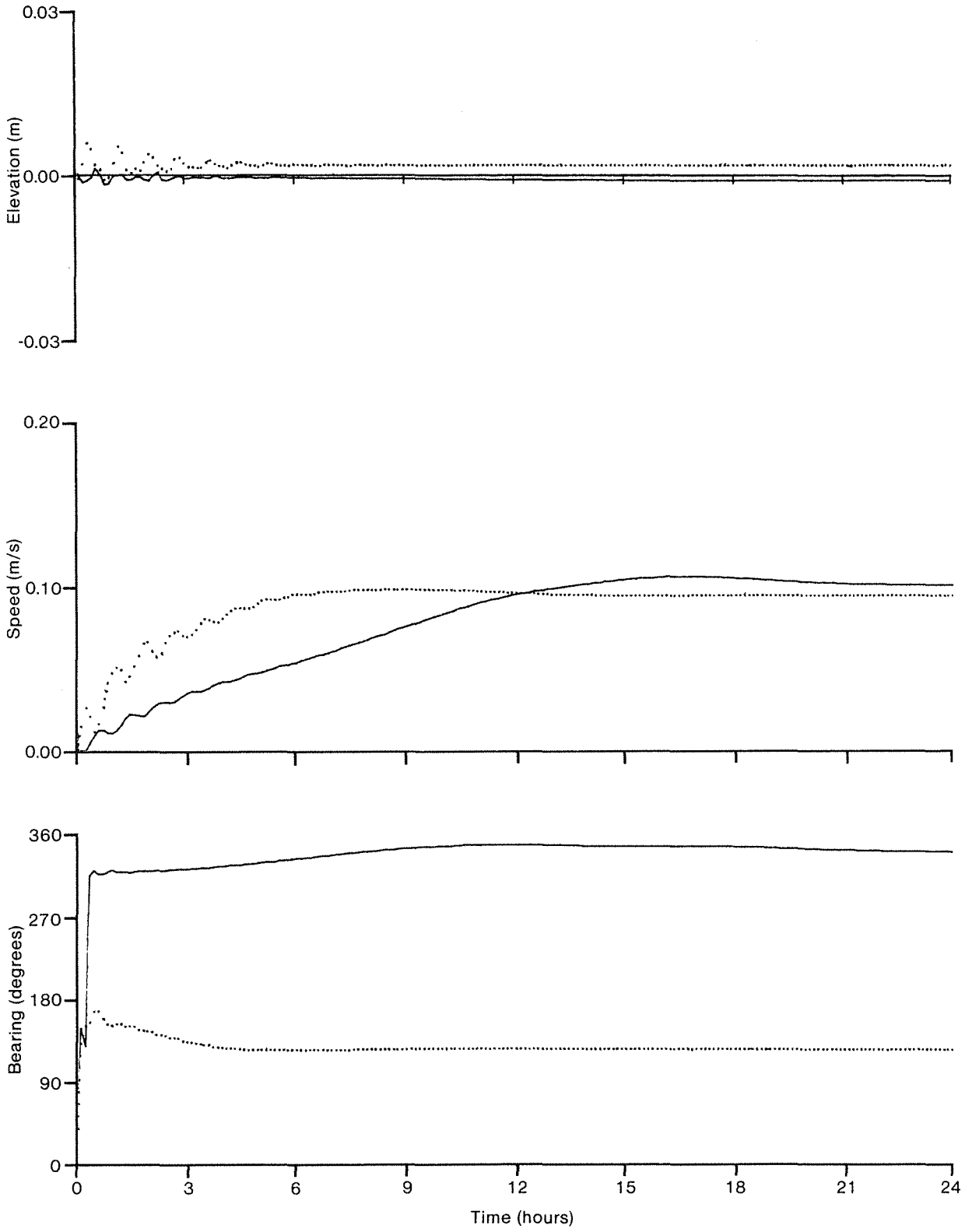

Figure C.2: Time-series of elevation, current speed and direction at cell 14,12 (————) and cell 4,12 (·····), 0-24 hours after the onset of a 0.1 Pa wind stress to the south-east.

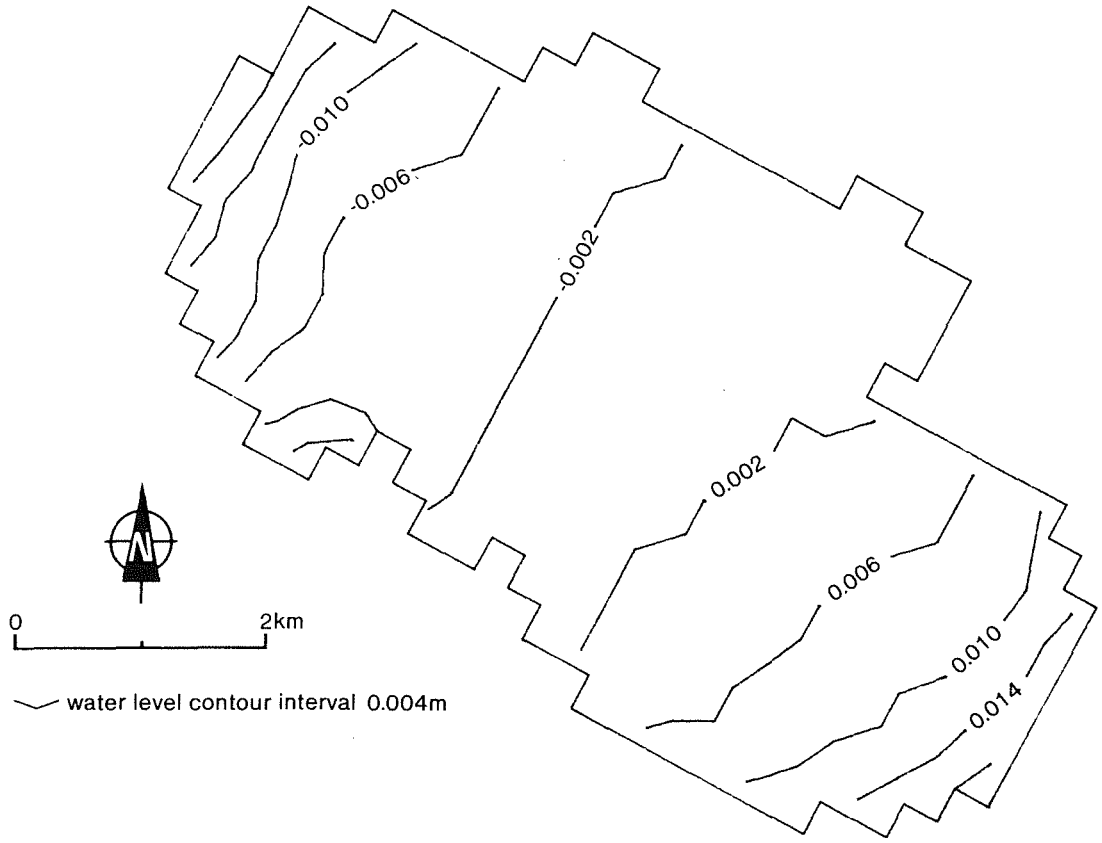

Figure C.3: Water level contours for a wind stress of 0.1 Pa to the south-east, 24 hours after onset of the wind.

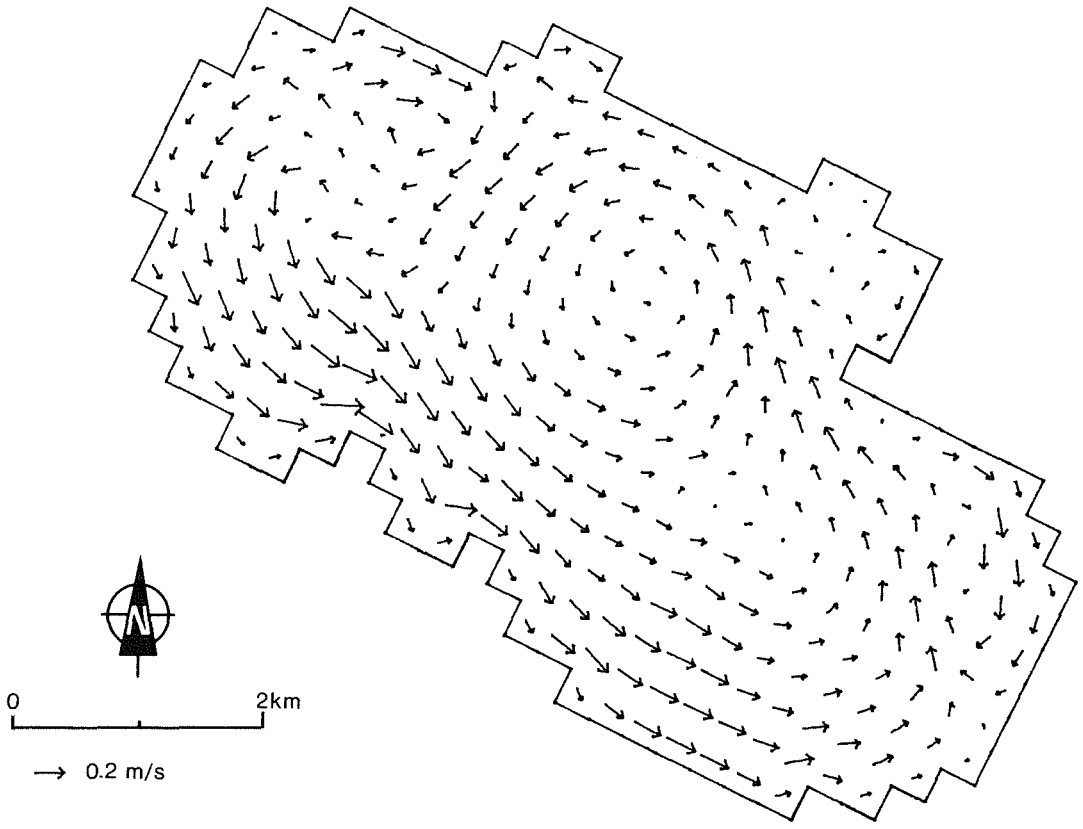

Figure C.4: Depth-averaged current velocity field for a wind stress of 0.1 Pa to the south-east, 24 hours after onset of the wind

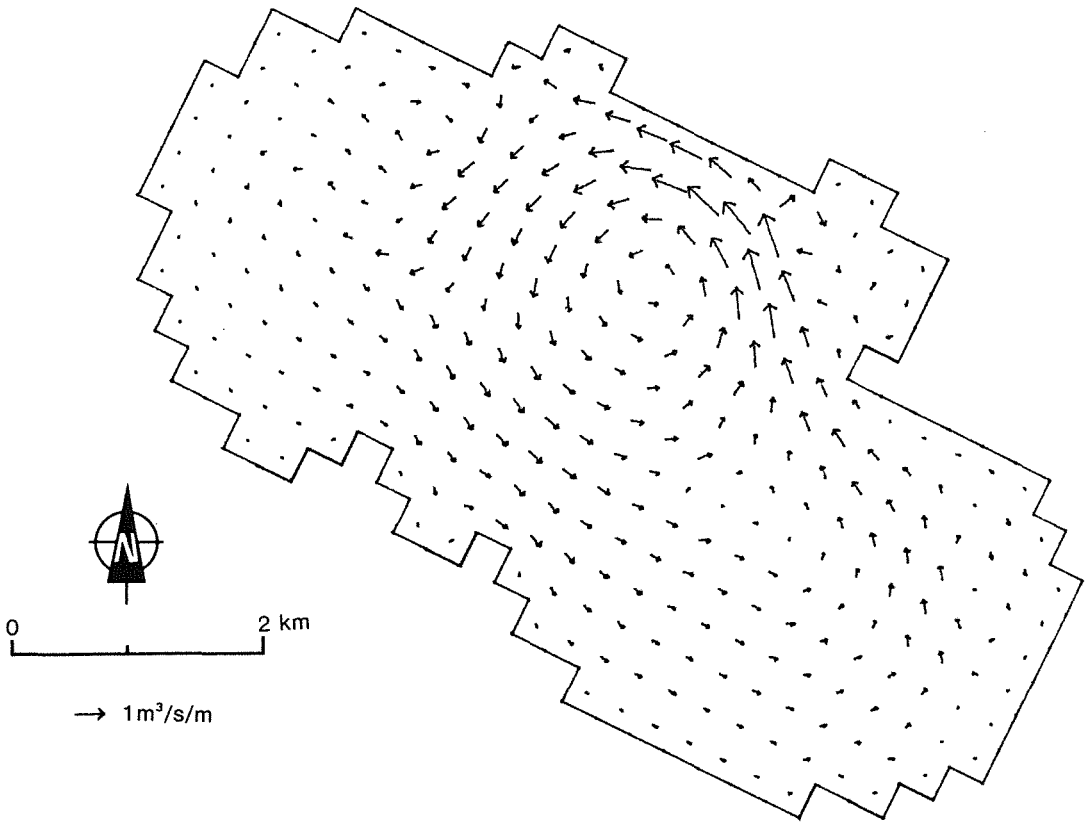

Figure C.5: Volume flow rate field for a wind stress of 0.1 Pa to the south-east, 24 hours after onset of the wind.

APPENDIX D

Model run D - Response to a Wind Stress of 0.1 Pa to the North-west

Model run D examined the response of PRH to a wind stress of 0.1 Pa in a north-westerly direction (corresponding to a wind speed of 8.5 m/s from the south-east).

Time-series plots of surface elevation and depth-averaged current speed and direction are shown in Figures D.1 and D.2 for the first 24 hours after the onset of the wind. The dominant seiching activity takes place along PRH, with a period of about 50 minutes. Surface level oscillations at the north-west and south-east ends of the harbour are large and opposite in phase (Figure D.1). Surface level oscillations are small across the width of PRH (Figure D.2). The current response at low frequencies is approximately exponential at all four grid cells for which time variations are presented. Establishment times for currents in the deepest areas of PRH are about 4 hours (Figure D.2).

Figure D.3 shows a contour plot of the water surface level at a time 24 hours after the onset of the wind. The contours are distributed similarly to those shown in Figure C.3, but the surface slope is in the opposite direction. Maximum water level differential is about 0.036 m.

Figure D.4 shows the depth-averaged current velocity field 24 hours after onset of the wind. The dominant feature is a clockwise circulation pattern which occupies most of PRH. The maximum water speed achieved is about 0.2 m/s. Minor gyres are present to the north and south-east of the harbour.

Volume flow rates for a south-east wind (Figure D.5) are similar to those for a north-west wind (Figure C.5), but with a clockwise rotation rather than an anti-clockwise rotation. Maximum volume flow rates occur in the dredged portion of PRH, adjacent to the wharf area.

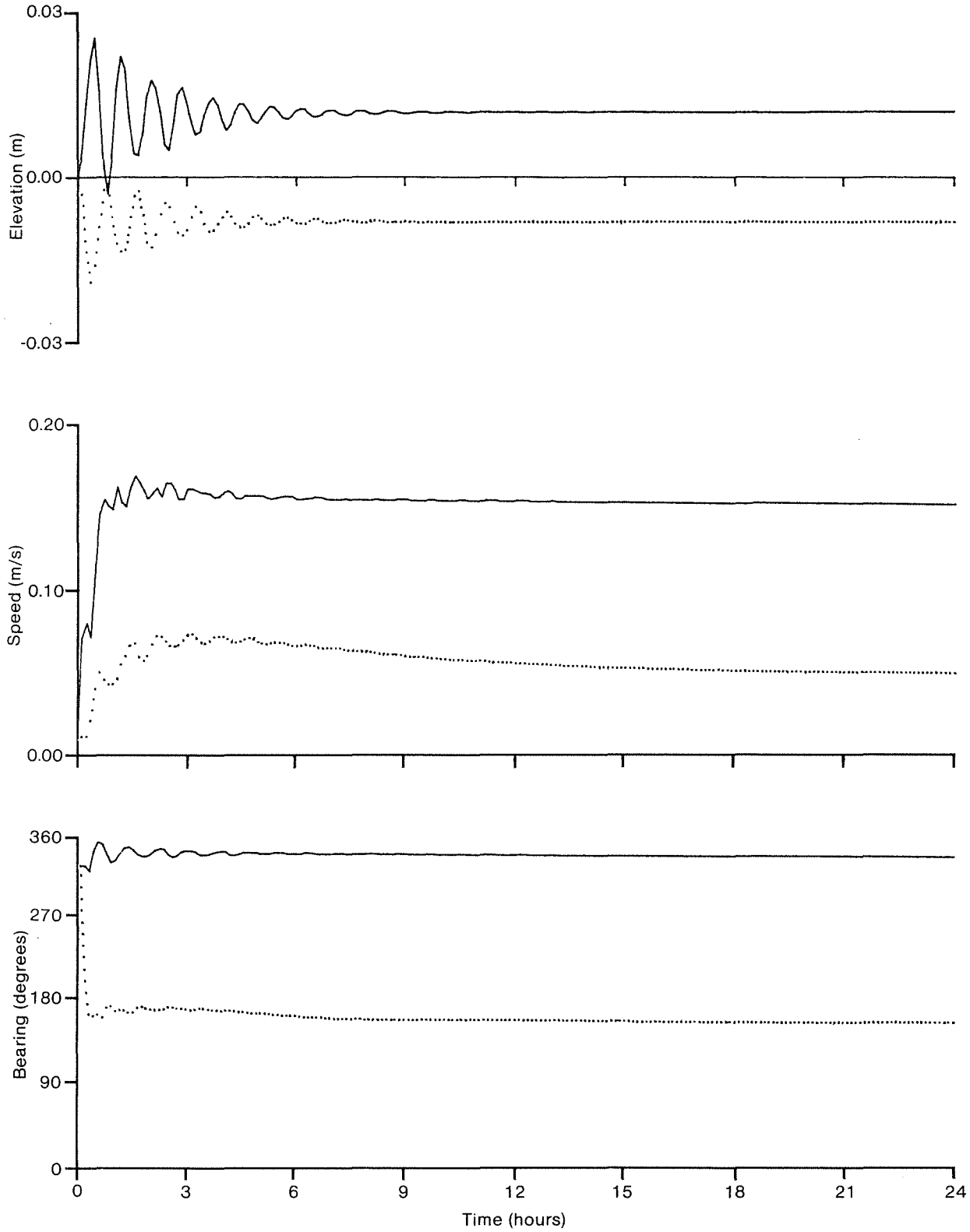

Figure D.1: Time-series of elevation, current speed and direction at cell 6,24 (————) and cell 7,4 (·····), 0-24 hours after the onset of a 0.1 Pa wind stress to the north-west.

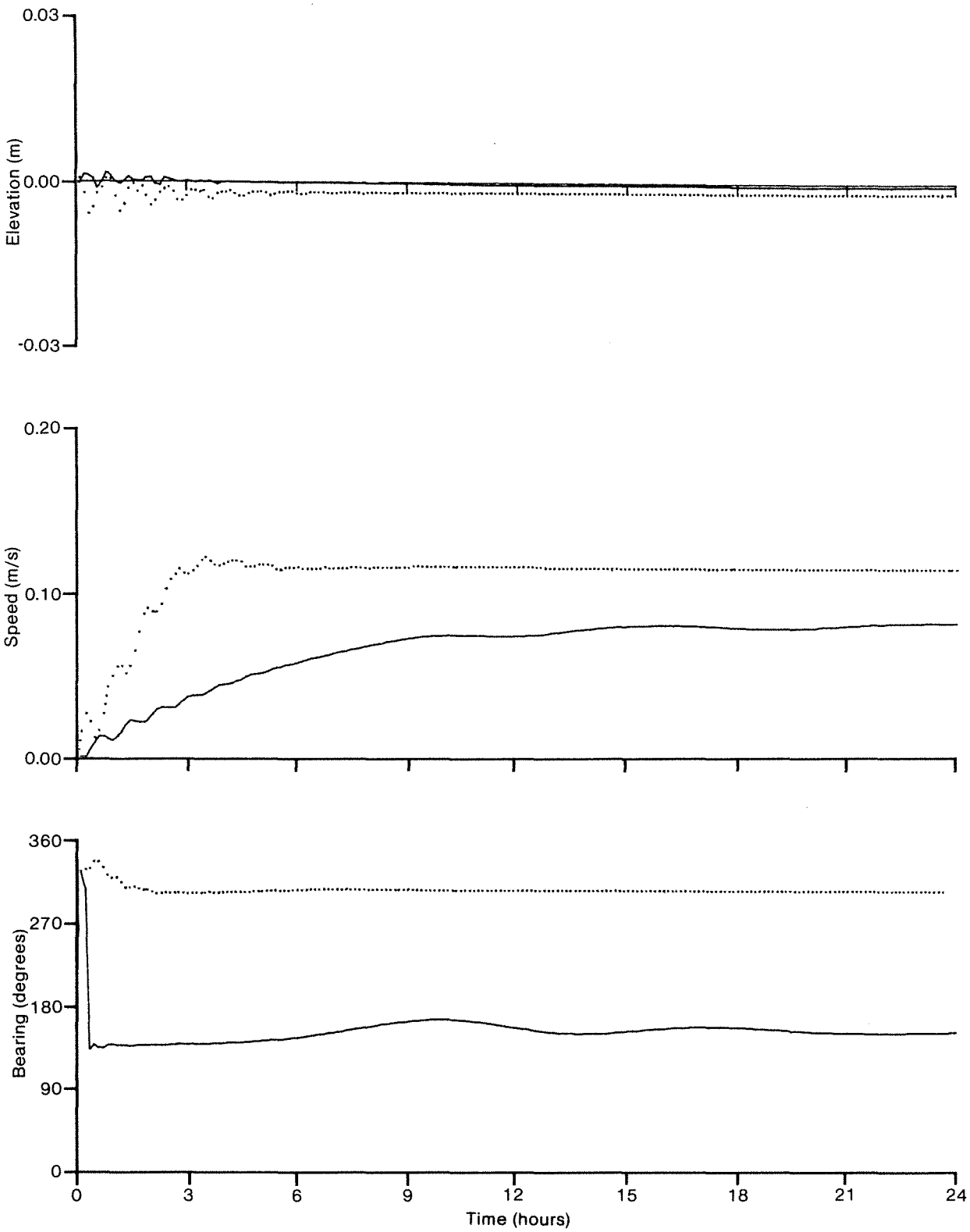

Figure D.2: Time-series of elevation, current speed and direction at cell 14,12 (————) and cell 4,12 (·····), 0-24 hours after the onset of a 0.1 Pa wind stress to the north-west.

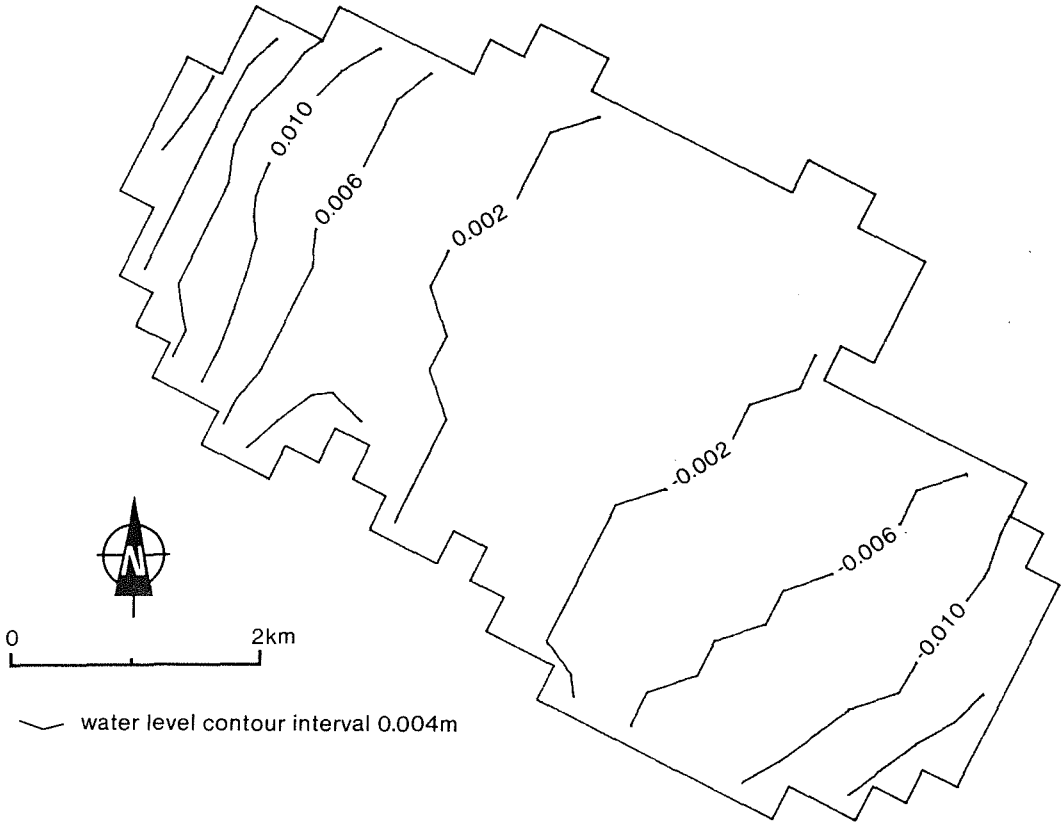

Figure D.3: Water level contours for a wind stress of 0.1 Pa to the north-west, 24 hours after onset of the wind.

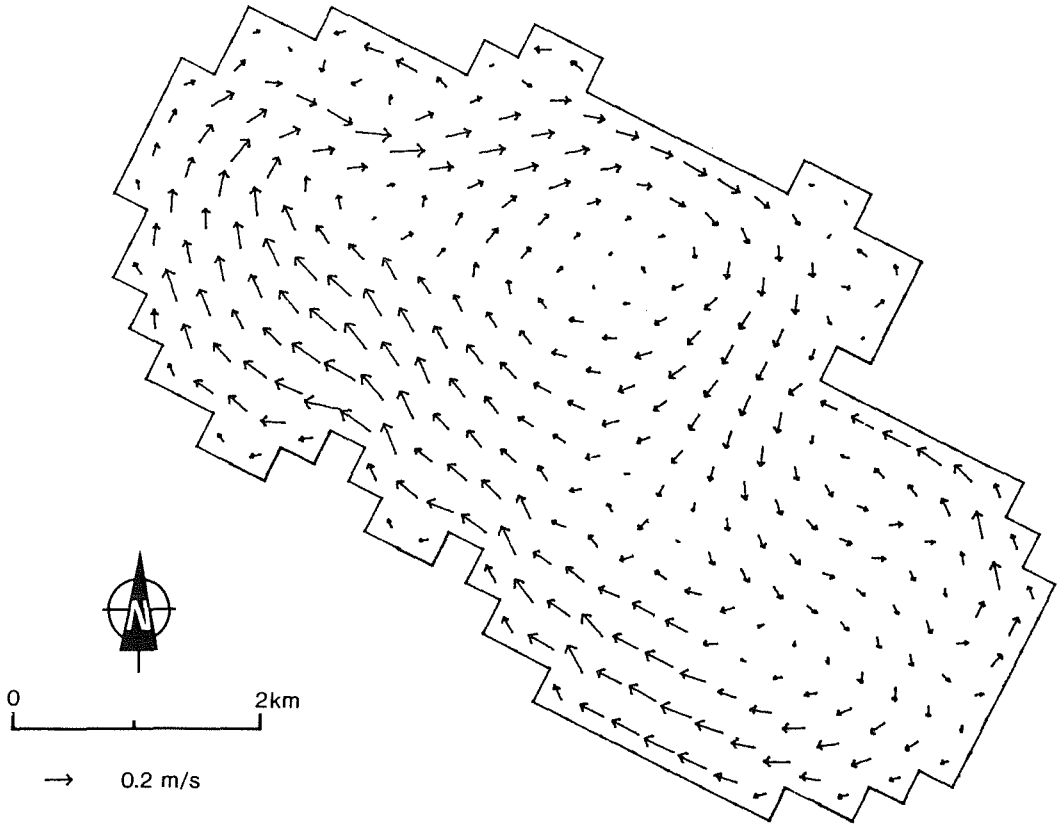

Figure D.4: Depth-averaged current velocity field for a wind stress of 0.1 Pa to the north-west, 24 hours after onset of the wind.

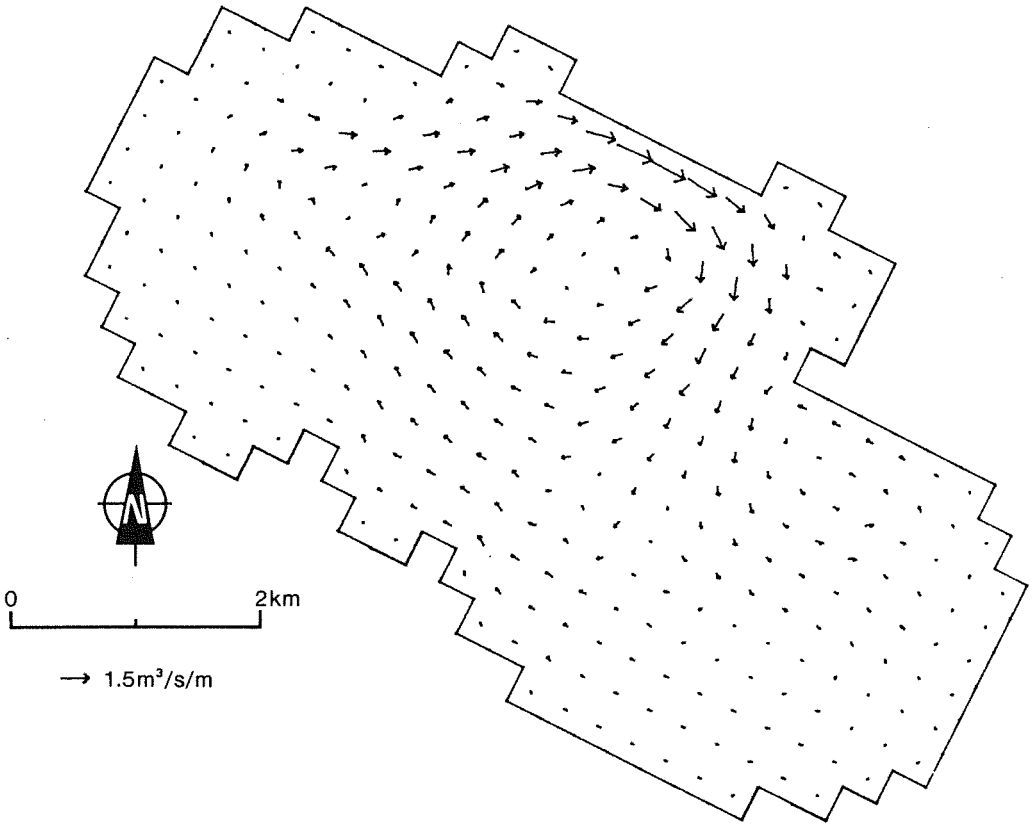

Figure D.5: Volume-flow rate field for a wind stress of 0.1 Pa to the north-west, 24 hours after onset of the wind.